Motor Mythbusters: Torque-producing force, The long version
By Peter Schimpf, P.E.

Abstract:

In describing how motor torque is developed, many textbooks incorrectly identify that the entire electromagnetic torque-producing force acts directly on the conductor. This is true only for simplified devices where the conductor is located in the airgap. But this is not true for most modern industrial motors where the conductors are located within slots in the iron core (for example induction motor rotors and stators). **When conductors are located in slots in an iron core, the electromagnetic torque-producing forces act primarily on the iron core.** There is some electromagnetic force acting on the conductors within slots, but it is primarily in the radial direction, rather than the tangential (torque-producing) direction.

Table of Contents (See bookmark tab at left for easy navigation)

Section 1   List Of Relevant Points

For summary purposes, I will break the above abstract into three "points" of discussion. These points will be proven later in this article.

    Point 1.   Many textbooks state or imply that the entire torque-producing electromagnetic force in modern electric machines acts directly on the conductors (vs the core). This is not true.   **With the**

conductors located in slots (as in a modern induction motor), the electromagnetic torque-producing force acts primarily on the iron rather than the conductor. [1]

Point 2. If we move a current-carrying conductor between the airgap and a slot (keeping current and airgap flux density the same) the total electromagnetic torque-producing force (on conductor and core combined) remains the same. (What changes is whether this force acts on the conductor or on the core iron).

Point 3. The electromagnetic force that does act on the conductors in slots while under load is primarily in the radial direction, rather than the tangential (torque-producing) direction.

Section 2   Why Is This Important?

As professionals working with electric motors on a routine basis, we would like to think that we have some idea of how a motor actually works, including the basic function of producing torque. Knowing what forces actually do and don't act on the conductors is important in motor design and post-mortem analysis of failed motors.

On the lighter side, if you mention at a gathering of motor professionals that the torque-producing force in industrial motors acts primarily on the iron core (rather than the copper conductors), I can almost guarantee that it will generate a lively discussion. In my experience, most people will react as if you had stated the earth is flat! The "myth" that the entire torque acts directly on the conductors is very widespread.

Section 3   Terminology/Basics

Subsection 3.1   Overview of motor construction

Figure 1 shows a simplified view of a motor highlighting the parts that we will be discussing. There is a rotating rotor within a stationary stator. Each has an iron core (shown in orange) which carries the magnetic flux and copper conductors (shown in green) which carry the electrical current. The conductors are put into slots within the iron cores. The slots are adjacent to the airgap on the outer diameter of the rotor core and the inner diameter of the stator core.

---

[1] The discussion of this paper refers to the portion of the conductor within the slots. There are also portions of conductors outside slots (vent ducts and end regions of rotor and stator) where the flux patterns and behavior are different, but these regions don't contribute much of the total motor torque and do not change the overall conclusion.

Figure 1 - Overview of motor parts (simplified)

Stator core

Stator conductor

Stator core slot

Rotor core

Rotor conductor

Rotor core slot
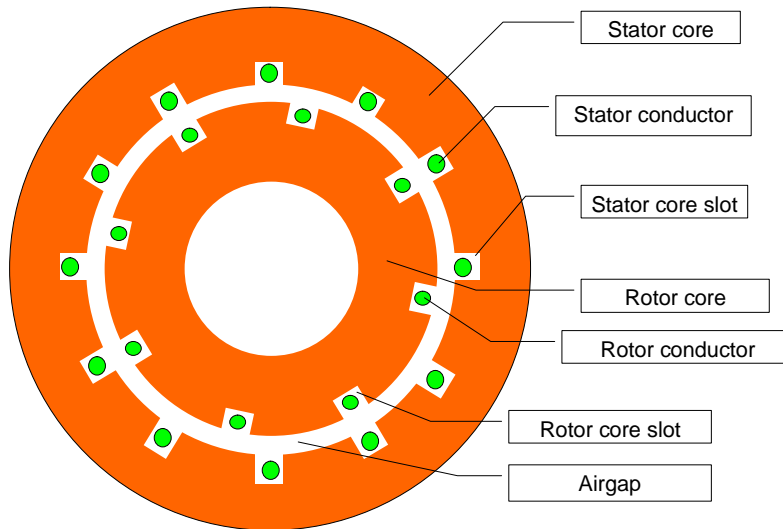
Airgap

Subsection 3.2   Commonly used symbols

B, b – magnetic flux density = flux /area (units: webers/m^2)
F – force (units: Newtons)
g – airgap dimension
H – magnetic field intensity - units (Amps/meters)
        (B and H are related by B =$\mu \cdot$ H)
i or I – current (units: Amps)
L - length of conductor   (units: meters)
L1, L2 – self-inductances (units: Henries)
M – mutual inductance
N – number of conductors
p – number of pole pairs in a motor
p.f. = power factor
R - radius from center of shaft to center of airgap
T - torque
v – velocity
V - volume
w – width of conductor loop (distance between the two conductors forming the sides of the loop)
w – magnetic energy density (w =W / V)
W – magnetic energy
x - linear position coordinate
x or x – vector cross product
α - electrical angle between B and I (section **Subsection 12.3**)
θ, β - angular position coordinate
Φ - flux (units: webers)
$\mathcal{R}$ - reluctance
μ - permeability – a property of the material.
$\mu 0$ – permeability of free space – applies to air and copper
μ_{iron} – permeability of iron ($\mu_{iron} \gg \mu 0$)
μ_r - relative permeability = $\mu / \mu 0$

⊗ - current flowing into the page (arrow tail)

⊙ - current flowing out of the page (arrow head)

🟧 = iron (orange used in my figures when possible)

🟩 = conductor (green used in my figures when possible)

🟦 = permanent magnet or flux-producing current loop (blue)

Subsection 3.3   Force on conductors - The Lorentz Force Equation and the Right-hand Rule

The Lorentz force equation for force on a current-carrying conductor in a magnetic flux is expressed in this paper as follows:

$$F = N\,L\,i \times B \quad \text{(we will assume N=1 in this paper)}$$

Equation 1

The following are equivalent alternate forms of the same Lorentz force relationship:

$$F = q\,v \times B$$
$$F = V\,J \times B$$

where F = electromagnetic force, q ,= charge, v = velocity, L = length of conductor, i = current, V = volume of conductor, J = current density, N = number of conductors.

The "$\times$" above indicates vector cross product. Assuming that the current is perpendicular to the flux, the magnitude is given by multiplication and the direction is given by the right hand rule for direction of force on conductors as shown in Figure 2.[2]

Figure 2 Right Hand Rule for direction of force on conductor

F=q(v x B)=L(I x B)

qv=LI

B

Right-hand rule:
v=direction of charge current
B = magnetic field
vxB = cross product
    = direction of the force
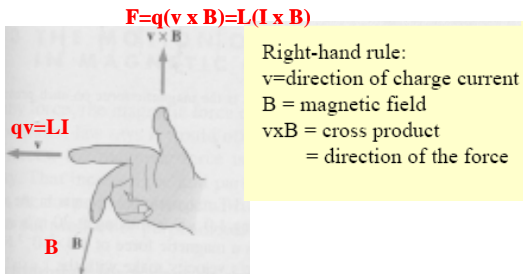
Subsection 3.4   Terminology for Directions

There are three directions we will use in the cylindrical motor geometry:
    tangential = parallel to airgap
    radial = perpendicular to airgap
    axial = parallel to shaft (for example current flows in axial direction)
See Figure 3 for further clarification of these terms

---

[2] The right-hand rule as described above is based on the "+ to -" current convention.

Figure 3 – Radial, tangential, and axial directions
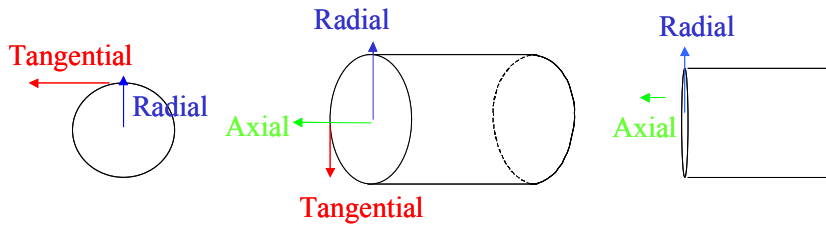
Section 4   Typical Simplified Textbook Explanation Of Torque Production

Below is an excerpt from reference 1 and associated figure which incorrectly implies that the torque-producing force in an induction motor acts directly on the rotor bars:

> *"The interaction of the magnetic field caused by the induced current in the squirrel-cage bars with the magnetic field of the stator. This force, for the instant shown in* [Figure 4]*, causes the rotor to experience a torque in the direction of the stator flux.8"*

Figure 4 Simplified explanation of torque production from reference 1
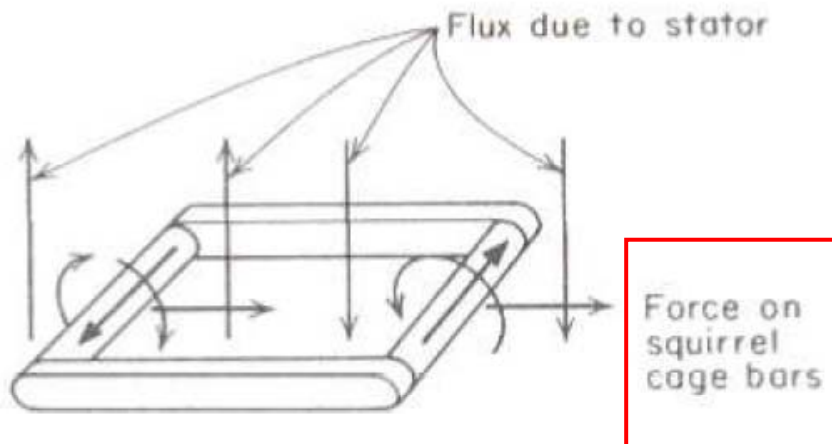
Note the unmistakeable annotion in the figure "<u>Force **on** squirrel cage bars</u>".[3]

There are many other similar explanations suggesting that the entire torque-producing force for motors acts directly on the conductors:

- Reference 2 states "The fundamental principle upon which electromagnetic motors are based is that there is a mechanical <u>force **on** any current-carrying wire</u> contained within a magnetic field"[3]
- Reference 3 states "''The rotating magnetic field induces emf in the rotor by the transformer action. Since the rotor is a closed set of conductors, current flows in the rotor. The rotating fields due to stator currents react with the rotor currents, <u>to produce forces **on** the rotor conductors and torques</u>."[3]
- Reference 4   states "The electromagnetic torque acting between the rotor and the stator is produced by the interaction of the main field Bd and the stator current density Ja, as a J **x** B <u>force **on** each unit volume of stator conductor</u>".[3]
- Reference 5 states "As is well known, the torque in any electric machine is caused by the <u>pull</u> of the magnetic field **on** <u>the current-carrying conductors</u>.[3]

---

[3] Emphasis added

While it is true that a conductor in a flux experiences a force in the direction shown, this is not the primary mechanism for torque production in modern induction motors with conductors located in slots.

Section 5   Seeing Is Believing (Video Demo)

I have prepared a video demonstration using a setup shown in Figure 5. A coil of wire is located within an iron slot. Both the coil and slot are suspended from above and free to swing left/right independently of each other.   Magnets are located above and below to provide a flux in the downward direction.   The demo is performed in two configurations: with and without the slot present.   When the current is applied without the slot present, the coil moves to the left as is fully expected and predicted by the Lorentz force law. But **when the slot is present around the conductor with current applied, the slot moves to the left and the conductor barely moves at all !**   This may be a surprising result for some people. The reasons for this behavior are the same reasons why the torque-producing force in a motor with conductors in slots acts primarily on the iron, rather than the conductor. These reasons will be made clearer later in this article.

Figure 5 - Equipment setup for the video demonstration
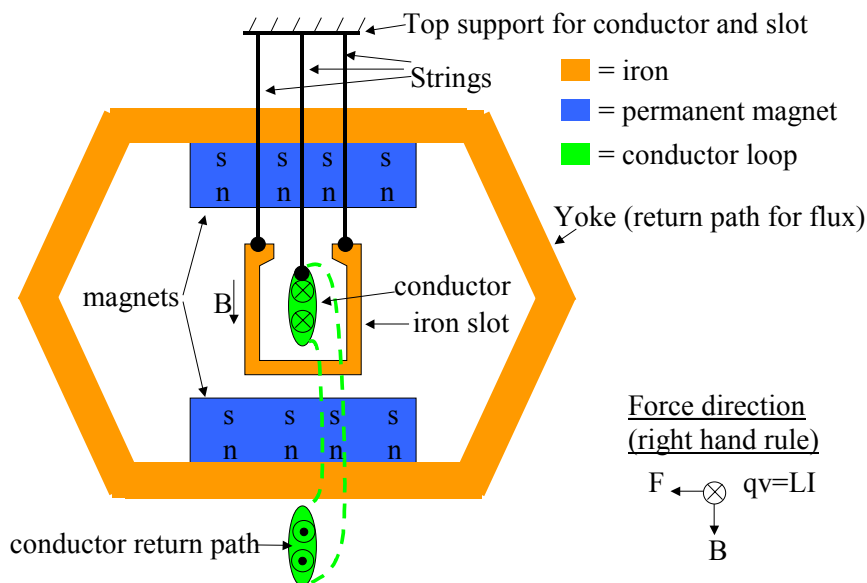
The video and more specific details about the demo construction can be accessed here:
http://home.comcast.net/~electricpete1/torque_web/videopage.htm
http://electricpete1.tripod.com/torque_web/videopage.htm

The flux and current in this demonstration are both dc. Someone people might believe that a static (dc) demonstration cannot tell us anything relevant about forces in a dynamic time-varying induction motor. I have no hesitation in stating that this dc demo does correctly reflect the behavior of forces associated with conductors in iron slots in ac machines.   The electromagnetic forces at a given point in time depend upon the current and flux distributions (along with geometry and permeability) at that point in time, but do **not** depend upon the time history or rates of change of these variables (for example, the Lorentz force method, the energy method, and the Maxwell Stress method all determine force from current, flux and geometry without any direct dependence on time).   Therefore, the force demonstrated in the dc demo represents a snapshot of the force on slot/conductor that would be seen in a time-varying ac system such as an induction motor at a point in time when the current and fluxes assume the values of current and flux used in the demonstration. Furthermore, if we varied the current and flux to represent conditions at a different point in time, the forces on both the conductor and the iron would scale linearly (to a first approximation, neglecting effects such as saturation). So we could vary the current and flux density in this demo as desired to represent any current and flux condition which might exist during normal operation of an induction motor, and the results for the

force on iron and conductor would both scale linearly by the same factor (the ratio between the two forces would remain the same, and therefore the force on the iron would always remain much larger).

Section 6   Description of flux lines:

Flux lines are widely used to provide a visual picture of the flux pattern within a machine.

At any given location in space, the magnetic flux lines tell the direction and relative magnitude of the flux density vector B. The direction of B is parallel to the flux lines. The relative magnitude of B is indicated by the density of lines. Where the lines are very close together, the magnitude of B is high; where the lines are spaced far apart, the magnitude of B is low.

Flux lines never intersect each other. They are roughly parallel to each other. Flux lines in air or copper next to iron (a highly permeable material) enter the iron at a right angle.   Additionally, flux lines tend to encircle the currents that create them as described for the right-hand-rule for flux direction (thumb in direction of current, fingers in direction of flux created by the current).

Most importantly, in the same way that electrical current follows the path of least "resistance", magnetic flux follows the path of least "reluctance" (reluctance is analogous to resistance – I'll use the terms interchangeably when the context is clear).   Iron presents a very low resistance to the flow of magnetic flux while air or copper present a very high resistance to the flow of flux.   When crossing an airgap, the majority of the flux lines will take the shortest path across the airgap from iron to iron. If there is a deep slot below the airgap, the flux lines will curve to find a short path to the iron.

This is illustrated in the finite element solution shown in Figure 6(a), which shows the flux pattern of a simple slot geometry (iron in orange, conductor in green, airgap in white) with an external flux applied, but no current in the slot.[4] We see that the flux lines generally do not travel directly through the slot, but jump across the narrow gap on each side of the slot instead.   Thus the flux density (B) is much lower in the slot section than in the airgap (as evidenced by the fact that the lines of flux are much further apart in the slot section than in the airgap).

Now let's think about what would happen about the above slot geometry if we removed the external flux but added current in the slot as shown in Figure 6(c).   The flux lines encircle the current in the direction given by the right-hand rule for flux-from current (thumb in direction of current, fingers point in the direction of flux from the current).   When leaving the iron, the flux takes the shortest path to encircle the current (straight across the airgap). There is a very small magnitude of flux which encircles a portion of the current by flowing tangentially across the slot (referred to as cross slot leakage flux).

Finally, we want to observe what happens when we include both current and external flux in the model as shown in Figure 6(e). We recall that the flux lines represent a map of the vector field at each point in space, where the direction is given by the direction of the lines and the relative magnitude is given by the density (closeness) of the lines.   The flux depicted in Figure 6(e) represents a vector sum of the fluxes in Figure 6(a) and Figure 6(c).   On the right side of the airgap we see that the external flux and the current flux are in the same direction and add together to produce a higher flux density (lines closer together). On the left side of the airgap, we see that the external flux and the current flux are in opposite directions, so the current flux subtracts from the external flux to create a lower flux density (lines further apart).   Additionally, viewing the radial airgap flux magnitude plot in the right-hand side of Figure 6, we can easily see that the airgap flux

---

[4] Note - The flux lines and flux magnitude plot shown in Figure 6, Figure 12, and Figure 14 were created from a finite element solution of the vector mangetic potential boundary value problem using the successive relaxation technique programmed in Matlab.   Powerpoint was used to add the arrows to clarify direction (not magnitude) of flux and the orange/green colors were added for clarification of the geometry.

profile of Figure 6(f) (current and external flux) represents the sum of the airgap flux profile from Figure 6(b) (external flux only) and Figure 6(d) (flux from slot current only).

Figure 6 – Flux-line plot and airgap flux plot for external flux only (a,b), current only (c,d), and total (e,f)

	Flux-line Plot	Radial airgap flux magnitude plot
External flux only (no current)	(a)	(b)
Current only (no external flux)	(c)	(d)
Current and external flux (combined)	(e)	(f)
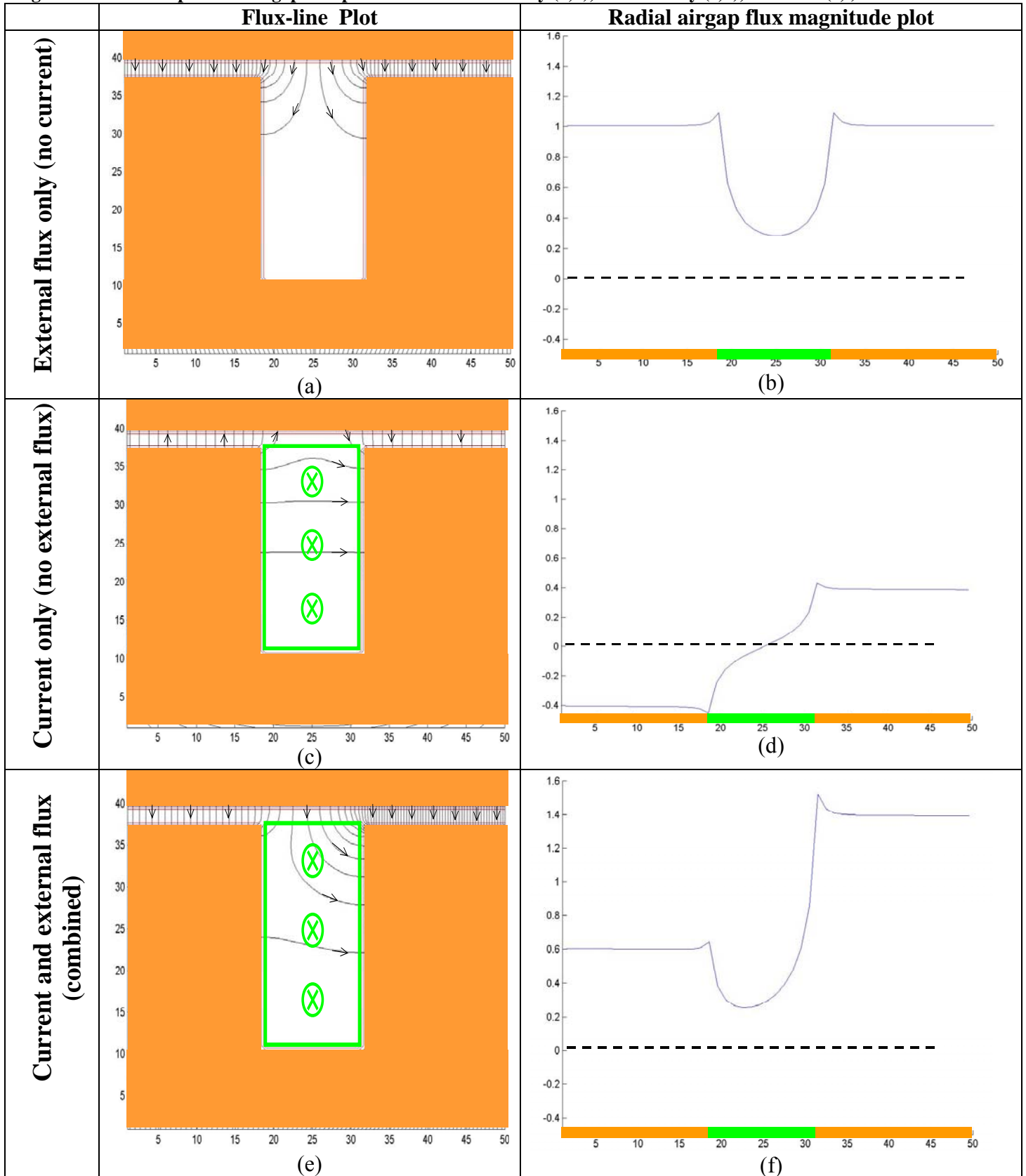
Flux plots also gives us a means to qualitatively visualize the force.   Reference 6 states *"Lines of B are useful for visualizing magnetic forces....This is a general rule: lines of B are 'under tension' and 'repel' laterally, just like lines of E"*.   Later (in Section 6) we will see that the forces associated with a magnetic field are related in a very straightforward manner to the energy stored in the magnetic field. The energy density is given by $w = 0.5 \cdot B^2/\mu$ (where w = energy per volume, B = flux density, μ = permeability). Therefore since the iron has very high permeability μ, the energy density within the iron is much lower than in the copper and air. Accordingly, when we apply the visualization procedure specified in reference 6, we should focus on the lines of flux in the air and copper, not in the iron. Therefore, I would restate the visualization rule as follows: *"The force created by a magnetic flux distribution can be determined qualitatively by considering the lines of flux in air or copper to act like stretched springs or rubber bands"*. This visualization technique allows us to qualitatively predict the force in many situations.

With this in mind, look first at Figure 6(e) which shows the combined flux from a current and an external uniform magnetic field. The flux density inside the iron does not contribute any significant energy since μ_iron is very large. The energy of the field resides in the slot and the airgap. Therefore we focus on the lines of flux in the air and slot acting like stretched springs. There is a vertical (radial) component of the flux which gives rise to a vertical (radial) force pulling the iron together. That radial force is the relevant force which if not balanced on the opposite side of an eccentric airgap would give us "unbalanced magnetic pull". But that radial force is not relevant for torque.   We also notice that there are more lines of flux entering the right wall of the slot than the left wall of the slot. Thus these lines of flux acting like stretched springs produce more leftward force on the right wall than rightward force on the left wall, and the resulting total horizontal (tangential) force on those two slot walls is to the left. This is the same direction we would expect from the right-hand rule for force acting on a conductor. But we may begin to suspect that the force is not acting directly on the conductor, since the radial flux density is very small within the slot section where the conductor is.   If a motor worked entirely on the principle of force directly on the conductor given by F=qV**x**B = NLI **x** B, then it would seem very counterproductive to put the conductors in the slots where the flux density B is the very low.

Section 7   The Energy Method for Calculating Electromagnetic Forces

While the Lorentz force equation (Equation 1) provides a very easy calculation for force appearing directly on the conductor, there is no comparably simple equation to define the force on general systems including materials with high magnetic permeability such as iron.

In this paper, we will use the energy approach for calculating the total electromagnetic force generated in a linear electromagnetic system, as given by the following two equations:

$$F = -\left[\frac{d}{dx}W\right]_{\Phi=\text{Constant}}$$

Equation 2

$$F = +\left[\frac{d}{dx}W\right]_{i=\text{Constant}}$$

Equation 3

where:

F is the electromagnetic force

W is the magnetic energy stored within the system

x is distance (F and x are positive in the same direction)

'Φ=Constant' denotes that the flux linkages are held constant when
evaluating the partial derivative of W with respect to x[Note 5]

'i=Constant' denotes that the currents are held constant when
evaluating the partial derivative of W with respect to x[Note 5]

The sign convention is that the positive direction for F is the same as the positive direction for x, and the positive direction for Φ is related to the positive direction for i by the right-hand rule for direction of flux from current (thumb in direction of positive current, fingers encircle the conductor in direction of positive flux).

Equation 2 can be shown by energy balance considering electrical energy input and mechanical energy output as in Figure 7:

Figure 7 – Simple input/output diagram for electromechanical system

where:

dW_{Mech} = increment of mechanical energy output from the system

dW_{Elect} = increment of electrical energy input to the system

dW_{Mag} = change in magnetic energy stored within the system

d = differential notation (similar to Δ)

An energy balance of the above system leads to

$dW_{Mag} = dW_{Elec} - dW_{Mech}$

The expression shown for dWelec can be found as follows:

$$\frac{dW_{Elec}}{dt} = P_{elec} = i(t) \cdot v(t)$$

Using the simplifying assumption of only one turn, we can substitute $v(t) = d\Phi/dt$

$$\frac{dW_{Elec}}{dt} = P_{Elec} = i(t) \cdot d\Phi/dt$$

If we look at the change in a small time period dt, we have

$dW_{Elec} = i \cdot d\Phi$

which is the expression shown in the figure above.

If we constrain Φ to be constant (as in Equation 2), then $d\Phi=0$ and $dW_{Elec} = i \cdot d\Phi = 0$ (no electrical energy is input), and the energy balance reduces to:

$dW_{Mag} = 0 - dW_{Mech} = - Fdx$

which is equivalent to Equation 2: $F = \dfrac{dW_{Mag}}{dx}$ (with Φ constant)

Equation 3 is not as straightforward to derive, since it does not exclude electrical energy input which may be required to maintain the current constant while changing the position.   But if we assume a simple system

---

[5] The choice of holding Φ or i constant has nothing to do with the behavior of Φ or i in the physical system.   Either choice when applied with its respective equation will give the same result.

characterized by $\Phi = L(x) \cdot i$, and associated energy $W = 0.5 \cdot L(x) \cdot i^2$, we can see that if $L(x)$ changes, then Φ and i must change in opposite directions from each other (we cannot hold both constant at the same time). We can show that Equation 2 and Equation 3 give the same result for the single-electrical input system as follows:

Using Equation 2:	Using Equation 3:
$F = -\left[\dfrac{d}{dx} W\right]_{\Phi=\text{Constant}}$	$F = +\left[\dfrac{d}{dx} W\right]_{i=\text{Constant}}$
$W = 0.5 \cdot L(x) \cdot i^2$	$W = 0.5 \cdot L(x)\, i^2$
To hold Φ constant, we need to rewrite W in terms of Φ by substituting $i^2 = \Phi^2/L^2$ as follows:	W is already in a format suitable for differentiation while holding i constant.
$W = 0.5 \cdot L(x) \cdot \dfrac{\Phi^2}{L(x)^2} = 0.5 \cdot \dfrac{\Phi^2}{L(x)}$	$F = +\left[\dfrac{d}{dx} 0.5 \cdot L(x) i^2\right] = 0.5 \cdot i^2 \cdot \dfrac{dL(x)}{dx}$
Use the chain rule for differentiation: ($[L^{-1}]' = -1\, L^{-2} L'$) as follows:	Substitute $i^2 = \Phi^2/L^2$:
$F = \dfrac{-d}{dx}\left(\dfrac{0.5 \cdot \Phi^2}{L(x)}\right) = \dfrac{+0.5 \cdot \Phi^2 \cdot \dfrac{dL(x)}{dx}}{L(x)^2}$	$F = +0.5 \cdot \dfrac{\Phi^2}{L(x)^2} \cdot \dfrac{dL(x)}{dx}$
	(This is the same result as with Equation 2)

The above has provided an example to show that Equation 2 (which we have demonstrated results from conservation of energy) and Equation 3 give identical results for the linear single-electrical input system. This also holds for multiple-electrical input systems (Proof is available upon request).

While a linear-motion expression for work (F dx) was used in the derivation above, a rotary-motion expression for work (T dθ, where T=torque) could have been used instead. This would lead in an obvious manner to an alternate form of Equation 2 and Equation 3 where T replaces F and θ replaces x.

The energy approach is well known and described in many textbooks. For example reference 7 states: *"Using the virtual work principle, the mechanical force in any direction is the partial derivative of the magnetic energy with respect to an incremental motion in that direction with the current held constant* [Equation 3]. *To find torque, differentiate with respect to the rotational angle."*

There are two approaches for applying the energy method to determine force: the *"field energy approach"* (used in Section 8 Section 9 and Section 13 and the *"circuit energy approach"* (used in Section 15 and Section 16. The *field energy approach* determines energy by integrating the energy density over the volume of interest. The *circuit energy approach* uses a circuit approach including self and mutual inductances to describe the energy within a system. Both approaches properly account for the energy and produce equivalent results. The field energy approach is more intuitive for those not familiar with circuits, but requires more algebra. The circuit approach seems to be preferred in most textbooks and allows an algebraically simpler solution since the self-inductance terms often don't vary with position x, and therefore these terms disappear when the derivative is taken.

When we evaluate the energy derivatives in Equation 2 and Equation 3, we can do it two ways: by analytically differentiating the algebraic expression for energy (Section 8 and Section 9) or by imagining a small movement Δx and analyzing the resulting change in the magnetic energy of the system (Section 13).

Section 8   Analysis Of Simple Pair Of Conductor Loops By The Field Energy Approach

Figure 8 - Simple Pair of Conductor Loops (sideview)
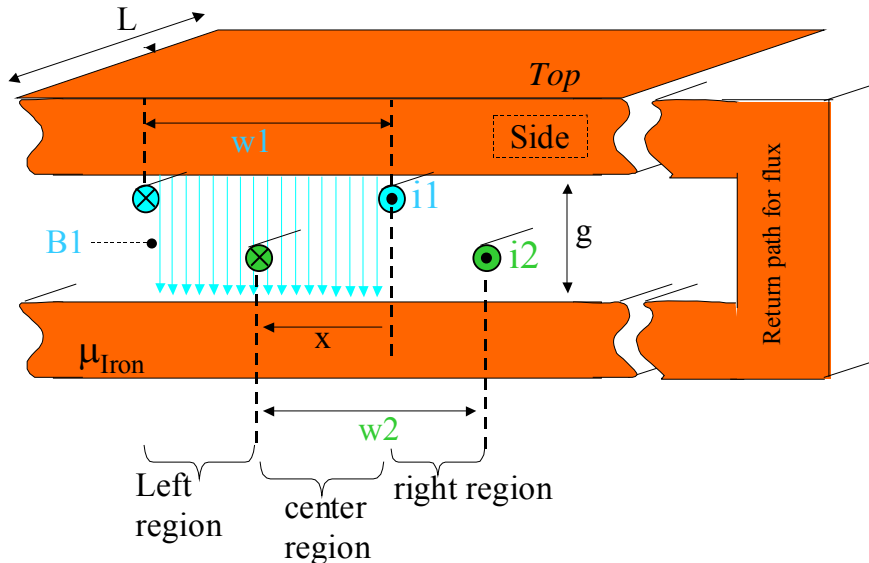
Figure 9 below is the same thing shown from a top view.

Figure 9 - Simple pair of conductor loops (top view)
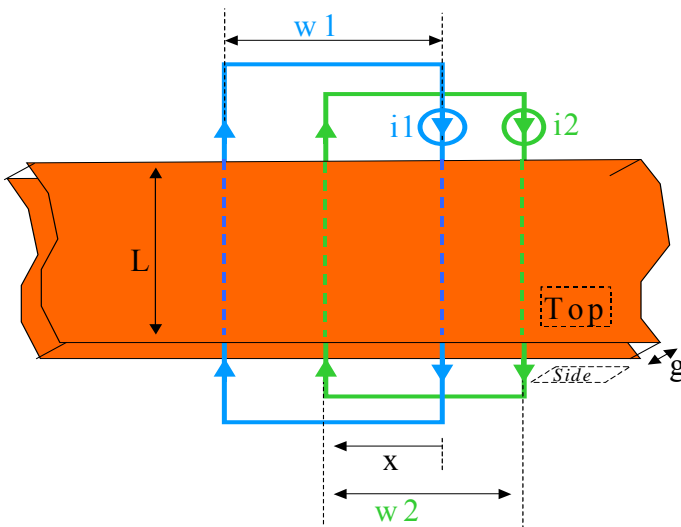
The symbols used in the analysis of Figure 8 and Figure 9 are as follows:

- g - gap dimension
- L - length of conductor within the flux (depth of core into the paper)
- w1 - width of loop 1
- w2 – width of loop 2
- i1 - this is the current in loop 1. We will use current i1 to create the flux B1. We will consider loop i1 to be a purely stationary flux-producing coil... we are not interested in the force on i1.
- i2 - this is the current in loop 2.   Loop 2 is the current upon which we will examine the electromagnetic force. The force occurs due to interaction of current i2 and flux density B1 (created by current i1).

- x - position of loop 2 (compared to loop 1) as shown on the figure. A change in x would correspond to movement of the entire loop 2 (both legs) as if it were a rigid coil. Note that only the left-most leg is within the flux B1 and only the leftmost leg of loop 2 will experience force.
- B1 - airgap flux density created by current i1
- b2 – airgap flux density created by current i2
- Left, center and right regions refer to regions of the airgap as indicated on the figure as follows:
  - "Left" - is the portion of the airgap that is inside loop 1 but outside loop 2
  - "Center" is the portion of the airgap that in inside loops 1 and 2
  - "Right" is the portion of the airgap that in inside loop 2 but outside loop 1

ASSUME $\mu_{Iron} \gg \mu 0$
ASSUME: gap dimension g very small. i.e. g << w1, w2, L

The above assumptions allow us to focus only on the vertical (radial) flux within the airgap and to neglect fringing or horizontal flux components.

The airgap flux density within conductor loop 2 can be calculated from Ampere's law (Integral H dot dl = μ_0 · Ienclosed) as follows:

$$b2 = \left(\frac{\mu_0 \cdot i2}{g} \right)$$ (note that this is discussed in more detail in Section 10).

B1 can be calculated in a similar manner to be $\left(\frac{\mu_0 \cdot i1}{g} \right)$, but we will not need this result.

We can express the flux densities in each of the three airgap regions in terms of the flux densities created by the individual current loops as follows:

B_{left} = B1
B_{center} = B1+b2
B_{right} = b2

We also know the volumes of each of the three regions.

V_{left} = (w1-x) · g · L
V_{center} = x · g · L
V_{right} = (w2-x) · g · L

We are now in a position to calculate the total energy. We start with the expression for energy density *w:*

$$w = \frac{B^2}{2\mu_0}$$

Since μ is very large in the iron, the energy stored in the iron is negligible and we only need to consider the energy stored in the airgap. The total energy (W) is determined from the sum of the products of the volume (V) of each region times the energy density (*w*) of that region as follows:

$$W = V_{left} \cdot w_{left} + V_{center} \cdot w_{center} + V_{right} \cdot w_{right}$$

$$W = V_{left} \cdot \frac{B_{Left}^2}{2\mu_0} + V_{center} \cdot \frac{B_{Center}^2}{2\mu_0} + V_{right} \cdot \frac{B_{Right}^2}{2\mu_0}$$

We simplify by pulling out common factors:

$$W = \frac{1}{2\mu_0} \cdot [V_{left} \cdot B_{left}{}^2 + V_{center} \cdot B_{center}{}^2 + V_{right} \cdot B_{right}{}^2]$$

Now plug in the volumes V:
$$W = \frac{1}{2\mu_0} \left[(w1 - x) \cdot g \cdot L \cdot B1^2 + x \cdot g \cdot L \cdot (B1 + b2)^2 + (w2 - x) \cdot g \cdot L \cdot b2^2 \right]$$

Simplify by pulling common factor g·L out of the brackets:
$$W = \frac{g \cdot L}{2\mu_0} \left[(w1 - x) \cdot B1^2 + x \cdot (B1 + b2)^2 + (w2 - x) \cdot b2^2 \right]$$

Now we find the derivative using Equation 3 (holding currents i1 and i2 constant will hold the associated flux densities B1 and b2 constant):
$$F = + \left[\frac{d}{dx} W \right]_{i1,i2,B1,b2=Constant}$$
$$F = \frac{g \cdot L}{2\mu_0} \left[-B1^2 + (B1 + b2)^2 - b2^2 \right]$$

Expand the square in the round parentheses:
$$F = \frac{g \cdot L}{2 \cdot \mu_0} \left[-B1^2 + (B1^2 + 2 \cdot B1 \cdot b2 + b2^2) - b2^2 \right]$$

Eliminating equal/opposite terms , we have:
$$F = \frac{g \cdot L}{2 \cdot \mu_0} \left[2 \cdot B1 \cdot b2 \right] = \frac{g \cdot L \cdot B1 \cdot b2}{\mu_0}$$

Substituting $b2 = \left(\frac{\mu_0 \cdot i2}{g} \right)$, we have:
$$F = \frac{g \cdot L \cdot B1 \cdot \left(\frac{\mu_0 \cdot i2}{g} \right)}{\mu_0}$$

Cancelling terms in numerator and denominator:
$$F = L \cdot i2 \cdot B1$$

Since F is positive, the direction of the force is in the direction of increasing x (to the left in Figure 8).

Thus using the energy method, we have determined that current i2 interacting with external flux density B1 sees a force exactly the same as we wold expect from Equation 1 (F = qv x B = L i x B). This should give us some confidence in applying the energy method in future sections.

Now in the next section, we will look at what happens if we place conductor loop 2 into a slot.

Section 9 Analysis of Simple Slot Geometry by Field Energy Approach

Figure 10 Simple slot geometry - field energy approach
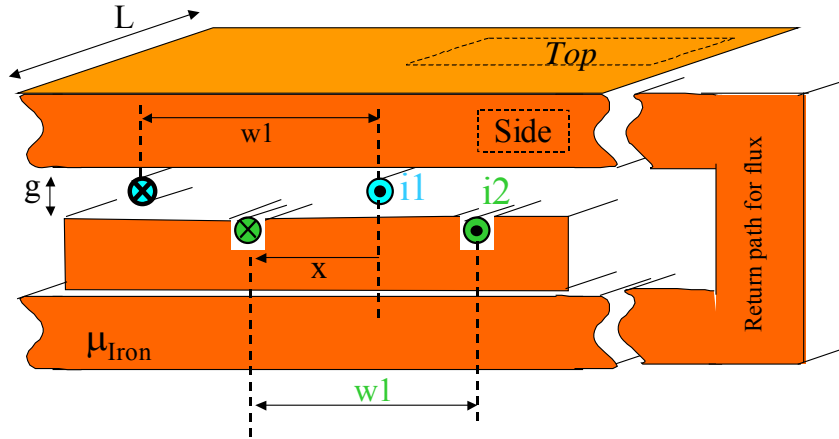
Figure 10 is similar to the simple pair of conductor loops shown in Figure 8, except that we have made it look more like a real motor by embedding both of the conductors of loop i2 in a slots within a horizontally-moveable iron piece. The conductors are assumed to be tightly fit into the slot so that the iron and conductors move together. All variables identified above remain the same except that x now represents the combined position of the conductor and moveable iron piece moving together.

B1 of course remains the same.

Application of Ampere's circuital law shows that b2 for this geometry (conductor in slot) remains the same as it was for the geometry of Section 8 (pair of conductor loops, no slot):

$$b2 = \mu_0 \cdot i2 / g$$

This may be surprising at first, but becomes obvious when we remember that the path length through iron does not affect the result (because we have assumed μ very large in the iron), and the distance to travel a closed loop in air across the airgap twice remains the same for either geometry. This is discussed further in Section 10 .

With all of the variables and relationships the same as before, we will naturally obtain the same result as before:

$$F_{total} = L \ i2 \ B1$$

...except that this time the force represents the **total** force (among conductor and the iron) since the x represents movement of the conductor and the iron together.

Section 10 Proof That The Total Torque-Producing Force For Conductor/Slot is the Same as For Conductor Directly in Airgap Flux (Proof Of Point 2)

First we will restate Point 2:

> *If we move a current-carrying conductor between the airgap and a slot (keeping current and airgap flux density the same) the total electromagnetic torque-producing force (on conductor and core combined) remains the same. (What changes is whether this force acts on the conductor or on the core iron).*

The proof is already given by examination of Section 8 and Section 9 . Specifically, these two sections examined the total force in the x direction, which corresponds to the tangential or torque-producing direction. And the results were:

- Section 8 demonstrated the tangential force acting on a conductor within an airgap is F=L I **x** Bgap.
- Section 9 demonstrated that the <u>total</u> tangential force associated with a conductor located within a slot is F=L I **x** Bgap.
  > where Bgap is the radial airgap flux density associated with the external flux (the flux not created by the current i2).

So the conclusion of Point 2 is already proven by examining the results above.

If we take a step back and look at how and why we reached this conclusion, we see that it arises from the surprising result that the airgap flux density created by current i2 was the same on both sides of the conductor, whether it was within the airgap or within the slot.   To understand this better, we will review how to determine the airgap flux density in both cases.

We determine flux density from Ampere's circuital law, which can be stated as follows:

$$\oint_C H \bullet d\ell = I_{Enclosed}$$

where:

H is magnetic field intensity, related to B by the equation: $B = \mu\, H$

$\oint_C$ indicates integration around a closed curve C

$I_{Enclosed}$ is the current enclosed by curve C

The curves which will be used for the above integration are shown in Figure 11.

Figure 11 – Curves for applying Ampere's Circuital law to conductor in airgap (a) and slot (b)
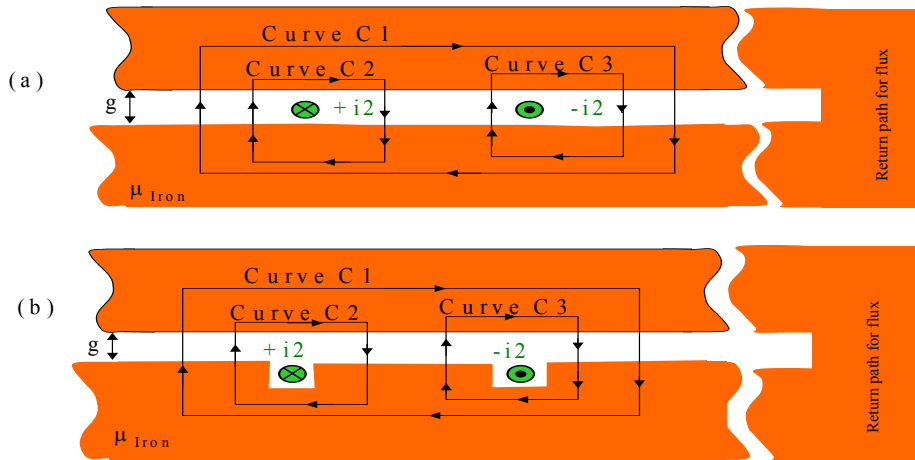
Since the permeability approaches infinity in the core section, the contributions to the integral in the core section will be negligible. This can be shown by observing that in the core region flux density B remains finite of comparable magnitude to the flux density in the air/conductor region. Therefore in the core region, the H is a factor of μ_r smaller. Since μ_r is very large in the core, H is very small in the core and its contribution to the integral is negligible.

Therefore, the only portions of the curve that will contribute to the integral are those within the airgap. There are three relevant sections of the airgap: to the left of the conductors, between the conductors, and to the right of the conductors. We will name the magnetic field intensity in these regions: Hleft, Hcenter, and Hright, respectively. We will declare the convention that H (and B) is positive when flux flows downwards in the airgap and i is positive when it flows into the page.

Applying the integral around Curve C1 (total current enclosed = 0), we have:

$-H_{left} \cdot g + H_{right} \cdot g = 0$

Applying the integral around Curve C2 (total current enclosed = i2), we have:

$-H_{left} \cdot g + H_{center} \cdot g = i2$

Applying the integral around Curve C2 (total current enclosed = -i2), we have:

$- H_{center} \cdot g + H_{right} \cdot g = -i2$

The above three equations are satisfied when $H_{left}=H_{right}=0$ and $H_{center} = i2/g$, noting that the fields from the two conductors cancel on the left and right sides since they are equal/opposite in these regions. And the airgap flux densities can be stated as $B_{left}=B_{right}=0$ and $B_{center} = \mu0 \cdot H_{center} = \mu0 \cdot i2/g$

The same logic applies whether we are looking at Figure 11(a) for a conductor in the airgap or Figure 11(b) for a conductor in a slot, and we end up with the same expression for airgap flux density B in either case. This should give some intuitive backup for the conclusion of this section. By knowing that the torque is transmitted across the airgap by the airgap flux pattern, and that the flux pattern is very similar for conductors in slots and conductors directly in the airgap, it should not be surprising that the total torque transmitted across the airgap is the same regardless of whether the conductor is placed in slots or in the airgap..

Finally, it is noted that references 8, 21, 25, 26, and 27 (excerpts included in Section 22) all support point 2. Some of those references don't say it exactly the way I have said it here. Some make the equivalent statement that we can calculate the total tangential force associated with a conductor/slot by substituting a flux density of Bgap into a force on conductor equation.

Section 11 Four-Step Proof That The Tangential Force In Simple Slot Geometry Acts Primarily On The Core

We now have all the tools we need to prove that the tangential force in the slot geometry acts primarily on the iron (vs. the conductor). We outline it in a simple four-step proof based on the geometry of Figure 10:

    #1:   Fconductor = L i2 Bslot
    #2:   Ftotal = L i2 Bgap
    #3:   Bslot << Bgap
    #4:   combining #1, #2, #3 shows Fconductor<<Ftotal and therefore the majority of the total force
            applies not on the conductor but on the core.

Note that Bgap represents the average of the radial airgap flux on both sides of the slot. Bgap plays the same role as B1 in the previous discussions.   Fconductor and Ftotal are the tangential (torque-producing) force on the conductor and the total (conductor plus iron).

Let us examine each of these areas in a little more details.

#1:   Fconductor = L i Bslot
      This is simple application of the Lorentz force law.   Note that Bslot is the flux density at the location of the conductor.

#2:   Ftotal = L i Bgap
      This was shown in Section 9   (except we have made the obvious substitution of i for i2 and Bgap for B1. Alternatively, we could have taken Point 2 (total force remains the same for conductor in airgap or in slot, as was proved in Section 10), and apply it to show that the total force on the conductor in slot is the same as if the conductor were in the airgap, which we know to be Ftotal=L i2 Bgap.

#3:   Bslot << Bgap

      The flux takes the path of least resistance from iron to iron. Therefore very little flux will travel the radially through the slot. We can see this looking at Figure 6(a) and Figure 6(e) above, where the flux lines are much further apart in the slot section than in the airgap (See note below for further discussion). And furthermore, what little flux does flow within the slot section is tangential and does not contribute to Bslot. (Bslot is defined as the radial flux density because it is the radial flux density that contributes to the tangential force on the conductor per the right hand rule for force on conductors).   Figure 12 shows a contour map of the radial flux densities associated with the finite element simulation of Figure 6(a).   The radial flux density in the airgap is 1.0.   At least half of the slot has an airgap flux density < 0.01 (1% of airgap radial flux density) and ¾ of the slot has a radial flux density of <0.1 (10% of airgap radial flux density).   We can easily conservatively guesstimate from this figure that the average radial flux density in the slot section for this particular geometry is 5% or less than the airgap radial flux density.

Figure 12 – Contour plot of radial flux density associated with Figure 6(a)
(NOTE that this is a contour plot, and not a field line plot)
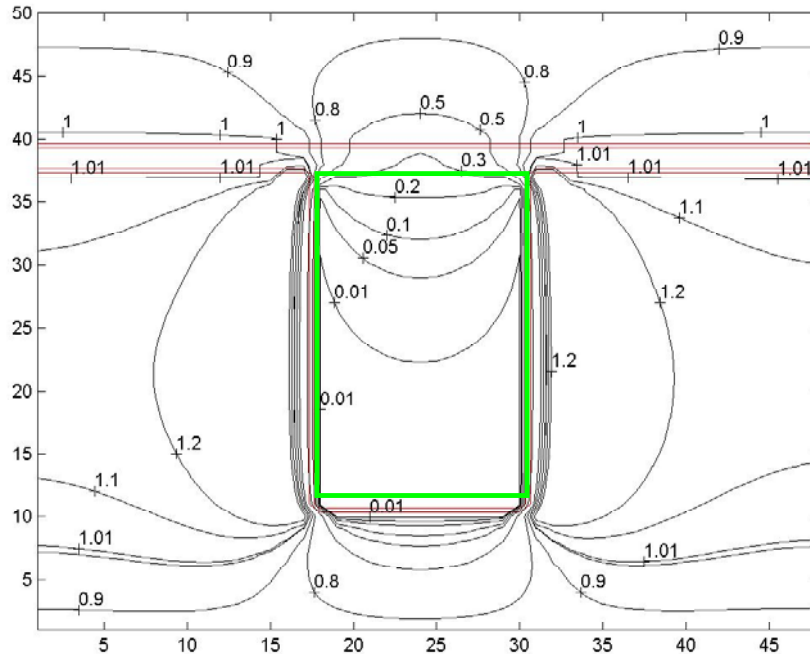
We can also get a rough estimate of the ratio Bslot/Bgap using the magnetic equivalent of ohm's law while neglecting fringing and saturation effects. This will tell us that Bslot/Bgap is inversely proportional to the distance the flux travels in air. If the airgap distance is g and the slot depth is d, the ratio would be Bslot/Bgap ~ g/(g+d). For typical slot and gap dimensions, this may be on the order of 1/20, indicating that the conductor force is only approx 5% of the total. The effect of fringing is to divert some the flux to the sides (vs. bottom) of the slot, which results in slightly higher flux density toward the top of the slot and lower flux density in the middle/bottom of the slot than would exist without fringing. We have also neglected any tooth saturation which may tend to increase slot flux density, but this is a small effect during normal full-load operation of an induction motor.

The above geometry represents an open slot (as may be seen in a form-wound stator). It should be obvious that a semi-closed slot or closed slot would give an even lower ratio of Bslot/Bgap.

Note - Where to look on Figure 6 to find Bslot and Bgap.
- Bgap – In Section 9 , B1 played the role of Bgap. B1 is the radial flux density created by conductor i1 on each side of the slot. We can see the relative magnitude of B1 by looking at the airgap region to the left and right of the slot in Figure 6(a).
- Bslot – Bslot is the flux density that will be plugged into the Lorentz force equation and as such should **in general** be the total flux density at the location of the conductor when it is carrying current (accordingly, it should be viewed in the slot section of Figure 6(e)). But in this particular case, we can use either the total slot flux density (Figure 6(e)) or the externally created slot flux density (Figure 6(a)) to plug into our force on conductor equation #1 (whichever is more convenient) and we will get the same result. The reason is that the flux created by the current itself (Figure 6(c)) does not exert any tangential force on the conductor due to the symmetry of this particular geometry (conductor centered within the slot and has no net force to the left or right in absence of external flux). A more formal justification follows: Since we have assumed linearity (no saturation), the the total force is the sum of the force due to the individual flux components. Let Bslot = Bslot1 + bslot2 where Bslot is total flux density (Figure 6(e)), Bslot1 is slot flux density due to external source i1 (Figure 6(a))and bslot2 is slot flux density due to the current in the slot itself i2 (Figure 6(c)). Then

Fconductor = L i2 Bslot = L i2 Bslot1 + L i2 bslot2.   But by the Lorentz force law, the quantity L i2 bslot2 is the tangential force created by the conductor itself in absence of any external flux, which we know is 0 from the symmetry. Therefore: Fconductor = L i2 Bslot = L i2 Bslot1. We can use either the total slot flux density Bslot (Figure 6(e)) or the externally created slot flux density Bslot 1 (Figure 6(a)) to calculate the force on the conductor.

In addition to the analysis provided above, there are numerous references confirming that Bslot << Bgap as identified in Subsection 12.5 .

#4:   Combining #1, #2, #3 shows Fconductor<<Ftotal
(and therefore the majority of the total torque-producing force acts on the core.)

This may be obvious, but in case it is not:
#1/#2 gives: Fconductor/Ftotal = (L i2 Bslot)/ (L i2 Bgap) = Bslot/Bgap
Fconductor/Ftotal = Bslot/Bgap
If Bslot<<Bgap (#3), then Fconductor<<Ftotal
The bulk of the total force does not act on the conductor, and must therefore act on the iron.

Section 12 Four-Step Proof That Torque-Producing Force In A Motor Acts Primarily On The Core (Proof Of Point 1)

Subsection 12.1   Overview of the four-part proof that torque-producing force in an induction motor acts primarily on the core:

The proof looks very similar to our previous four-part proof:
#1 - Tconductor = R· N ·I· L· Bslot· pf
#2 - Tmotor = R· N ·I· L· Bgap· pf
#3 - Bslot << Bgap
#4 - Combining 1 thru 3 proves Tconductor << Tmotor

where the symbols used above are defined as follows:
N = number of conductors
L = length of each conductor in the slot section
I = rms value of the fundamental current in each conductor
Bslot is rms of the fundamental radial flux density in the slot section
Bgap is rms of the fundamental radial flux density in the airgap
p.f. is cosine of angle between B and I which represents a power factor
Tmotor = total motor torque (sum of conductor torque and iron torque)
Tconductor = torque created by force acting directly on the electrical conductors
R = radius.   R is radius from center of the motor to conductor for #2 and to airgap for #1. We will assume these are approximately the same.

Subsection 12.2   Proof that Point 2 (equivalence of total force for conductor in airgap or slot) remains valid for rotary geometry of a motor.

Figure 13 - simple two-conductor loop rotary problem
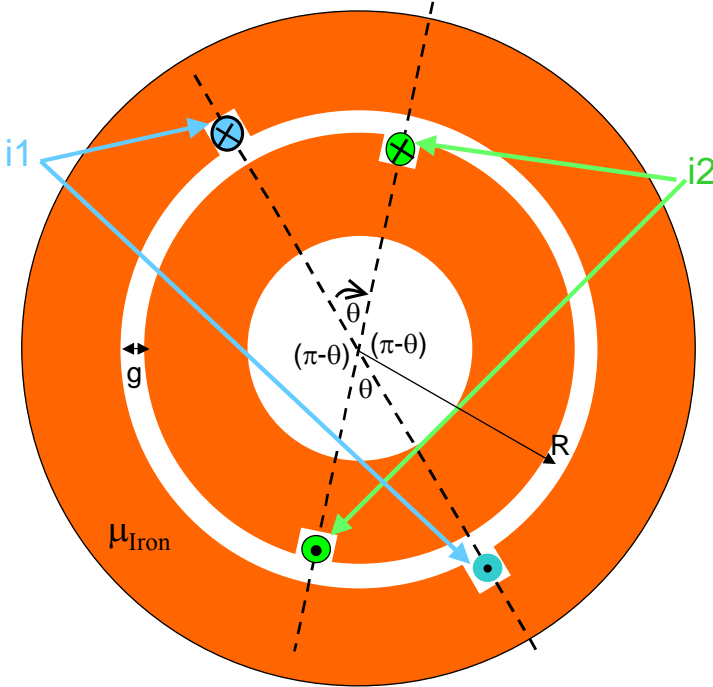
We begin by examining Figure 13.   We again have a current loop i1 which can represent the exciting component of stator current and current loop i2 which can represent a rotor conductor. [6]

We will define the convention that flux is positive when it flows inwards. As can be shown from Ampere's circuital law, the airgap flux density created by loop 1 is:

$$B1(\beta) = \begin{cases} +\mu 0 \cdot i1/(2g) = +B1 & \text{to the right of loop i1} \\ -\mu 0 \cdot i1/(2g) = -B1 & \text{to the left of the loop i1} \end{cases}$$

And the airgap flux density created by loop is similarly:

$$b2(\beta) = \begin{cases} +\mu 0 \cdot i2/(2g) = +b2 & \text{to the right of the loop i2} \\ -\mu 0 \cdot i2(2g) = -b2 & \text{to the left of the loop i2} \end{cases}$$

where the functional notation $B1(\beta)$ and $b2(\beta)$ denote that these variables depend on the location within the airgap. Angular coordinate β is not explicitly shown on the drawing since the regions of interest can be adequately described without it.

Proceeding in a similar manner as before, we notice that there are four regions of the airgap: left, top, right, bottom.   The boundaries between these four areas occur at the conductors.

Knowing the flux densities associated with the individual loops, we know the flux densities in each of the four airgap regions as follows:

$$B_{right} = B1 + b2$$
$$B_{left} = -B1 - b2$$

---

[6] If we wanted to model the stator load current component in analysis of Figure 13, we would include a current of magnitude (-i2) in the stator directly accross the airgap from loop i2. This extra complication is not required because the interaction between rotor conductor i2 and the equal/opposite adjacent stator load current component produces zero torque.

$B_{top} = B1-b2$

$B_{bottom} = -B1+b2$

We know the energy densities in these regions w=W/Volume = $\dfrac{B^2}{2\mu_0}$

$w_{right} = \dfrac{(B1+b2)^2}{2\mu_0}$

$w_{left} = \dfrac{(-B1-b2)^2}{2\mu_0} = \dfrac{(B1+b2)^2}{2\mu_0} = w_{right}$

$w_{top} = \dfrac{(B1-b2)^2}{2\mu_0}$

$w_{bottom} = \dfrac{(-B1+b2)^2}{2\mu_0} = \dfrac{(B1-b2)^2}{2\mu_0} = w_{top}$

Noting the symmetry in energy density (top same as bottom and left same as right), we will combine the top/bottom regions and we will combine the left/right regions during further analysis.

We also know the volumes of these regions:

$V_{top/bottom} = 2\cdot\theta\cdot R\cdot g\cdot L$

$V_{left/right} = 2\cdot(\pi-\theta)\cdot R\cdot g\cdot L$

(where R is radius of the airgap, g is airgap distance, L is length)

We are now in a position to calculate the total energy. Since μ is very large in the iron, the energy stored in the iron is negligible and we only need to consider the energy stored in the airgap. The total energy W is determined from the sum of the products of the volume of each region times the energy density of that region as follows:

$W = V_{left/right}\cdot w_{left/right} + V_{top/bottom}\cdot w_{top/bottom}$

Plug in values for V and w as follows:

$W = 2\cdot(\pi-\theta)\cdot R\cdot g\cdot L\cdot\dfrac{(B1+b2)^2}{2\mu_0} + 2\cdot\theta\cdot R\cdot g\cdot L\cdot\dfrac{(B1-b2)^2}{2\mu_0}$

Simplify by pulling out common factors:

$W = \dfrac{R*g*L}{\mu_0}\cdot[\ (\pi-\theta)\cdot(B1+b2)^2 + \theta\cdot(B1-b2)^2\ ]$

Now we find the torque as the derivative with respect to θ using Equation 3 (holding currents i1 and i2 constant will hold the associated flux densities B1 and b2 constant)

$T = +dW/d\theta$ (i1,i2,B1,b2 constant)

Computing the derivative with respect to θ of the expression for W, we have:

$T = (R\cdot g\cdot L/\mu_0)\cdot[\ -(B1+b2)^2 + (B1-b2)^2\ ]$

expanding the squares, we have:

$T = \dfrac{R*g*L}{\mu_0}\cdot[\ -(B1^2 + 2B1b2 + b2^2) + (B1^2 - 2B1b2 + b2^2)\ ]$

Removing equal/opposite terms, we have

$$T = \frac{R*g*L}{\mu_0} \cdot [\ -(2 \cdot B1 \cdot b2)\ + (-2 \cdot B1 \cdot b2)\ ]$$

$$T = -4 \cdot R \cdot g \cdot L \cdot B1 \cdot b2 / \mu 0$$

Substituting b2 $= \mu 0 \cdot i2 / (2 \cdot g)$, we have:

$$T = -2 \cdot R \cdot L \cdot B1 \cdot i2$$

This is exactly the same as we would have predicted from Equation 1 (F=L i2 **x** B1). The factor of 2 accounts for the fact that there are two sides of loop i2, both experiencing force. The factor of R converts force to torque. The negative sign indicates that the torque acts in a direction to decrease theta (to the left on the upper leg of loop i2), which is in agreement with the right hand rule for direction of force. The force associated with conductor loop i2 in this geometry is the same as it would have seen if it were in the airgap exposed to flux +B1 (at the top leg of i2) and –B1 (at the bottom leg of i2). The relevant dimension R is associated with the location of the airgap (not the conductors).

We have proven that Point 2 (equivalence of total force for conductor in airgap or slot) applies to the rotary geometry shown in Figure 13. We now turn to the individual elements of the four-part proof.

Subsection 12.3   Part #1 of 4-part proof: Tconductor = R · N · I · L · Bslot ·pf

Overview of #1 derivation. The following derivation comes from the basic relation for force on a conductor F = q v **x** Bslot = L I **x** Bslot. Since the physical angle between I (axial) and B (radial) is 90 degrees, the vector cross product becomes a scalar multiplication. This gives F = L I Bslot. When we sum the contribution of all the conductors, we have to account for the phase shift between the sinusoidally distributed I and Bslot in the same way that we account for the angle between voltage and current by adding a cosine of the angle between them which we call power factor giving F = N L I Bslot p.f.. To arrive at the final equation we convert force to torque using the radius T = R F = R N L I Bslot p.f.   We assume that the currents are sinusoidally distributed and neglect the winding and pitch factors.

Detailed derivation of #1:

Let the radial flux density in the slot be given by

$$Bs(\theta, t) = Bs_{max} \cos(p \cdot \theta - w \cdot t)$$

Where

Bs(θ,t) is radial flux density in the slot
Bs$_{max}$ is the max value of Bs(θ,t)
θ is mechanical angle
p is the number of pole pairs in the machine
w is the radian time frequency of the fundamental field $= 2\pi \cdot 60hz$
t is time

We have a distribution of currents within the conductors at N discrete locations which vary in magnitude approximately sinusoidal around the circumference.

$$Ic[k, t] = Imax \cos\left(p \cdot k \cdot \frac{2\pi}{N} - \alpha - w \cdot t\right)$$

Where:

> N is the number of conductors
> k is index for the kth conductors. k goes from 1..N
> $Ic[k,t]$ is current in the kth conductor at time t
> Imax is the maximum current.
> p is the number of pole pairs in the machine
> α is the electrical or time angle between flux and current peaks
> α/p is the mechanical angle between flux and current peaks

As N gets very large, the location of the conductors gets closer together, and we can approximate the discrete distribution of current $Ic[k,t]$ at any moment in time as a continuous distribution of current $\lambda c(\theta,t)$ at the same moment in time:

$$\lambda c(\theta, t)ds = \lambda max \cdot \cos(p \cdot \theta - \alpha - w \cdot t)ds$$

> where:
> θ is the mechanical angle coordinate
> $p \cdot \theta$ is the electrical angle
> $\theta \sim k \cdot (2\pi/N)$ gives the mapping between k and θ
> ds is the differential distance around circumference (ds=R·dθ)
> $\lambda c(\theta,t)ds$ = continuos approximation of $Ic[k,t]$
>> (λc is current density per length of rotor circumference in units of amps/meter)
> λmax = peak of the current density λ

In order to find the relationship between Imax and λmax, we will require that the total current over any sufficiently large arc is approximately the same for $Ic[k]$ and $\lambda c(\theta)$. Specifically we will require:

$$\sum_{k=k1+1}^{k2} Imax \cdot \cos\left(p \cdot k \cdot \frac{2\pi}{N} - \alpha - w \cdot t\right) = \int_{s=k1 \cdot \frac{2\pi R}{N}}^{k2 \cdot \frac{2\pi R}{N}} \lambda max \cdot \cos(p \cdot \theta - \alpha - w \cdot t)ds$$

Where on the left side sum, we have excluded the lower endpoint and included the upper endpoint as a simple approximate means of addressing the difference between continuous and discrete endpoints. A more exact approach would have used half of both the upper and lower endpoints , but this is not necessary considering that treatment of endpoints is less important for larger intervals k2-k1.

The sum on the left side of the above equation is difficult to evaluate. However, an alternate approach can be taken using a more general form of the equation which results from letting the function f(x) represent cos(px-α-w·t)

$$\sum_{k=k1+1}^{k2} Imax \cdot f\left(k \cdot \frac{2\pi}{N}\right) = \int_{s=k1 \cdot \frac{2\pi R}{N}}^{k2 \cdot \frac{2\pi R}{N}} \lambda max \cdot f(s)ds$$

Based on the known relationship between s and k (θ=k·2πR/N), we expect that if N is large enough, the above equivalence should hold true for any reasonably smooth function f. Therefore, for sole purpose of evaluating the relationship between Imax and λmax, we will choose the simple function f(x)=1.

$$\sum_{k=k1+1}^{k2} Imax \cdot 1 = \int_{s=k1 \cdot \frac{2\pi R}{N}}^{k2 \cdot \frac{2\pi R}{N}} \lambda max \cdot 1 ds$$

$$(k2 - k1) \cdot \text{Imax} = (k2 - k1) \cdot \frac{2\pi \cdot R}{N} \cdot \lambda\text{max} \cdot$$

$$\text{Imax} = \frac{2\pi \cdot R}{N} \lambda\text{max}$$

$$\lambda\text{max} = \text{Imax} \cdot \frac{N}{2\pi \cdot R}$$

We will use this resulting value for λmax later.

Force on the kth conductor can be given from Fc=q V **x** Bs = L I **x** Bs

$$Fc[k,t] = L \cdot Ic[k,t] x\ Bs\left(\theta = \frac{k2\pi}{N}, t\right)$$

where

Fc[k,t] is force on the kth conductor
L is the active length (in the slot section) of the conductor
x represents cross product
Bs(θ=k2π/N,t) is Bs(θ) evaluated at the point θ=k2π/N

Recognizing that Bs (defined as **radial**) is perpendicular to I (which is axial), we can remove the cross product (the resulting force will be in the tangential torque-producing direction)

$$Fc[k,t] = L \cdot Ic[k,t] \cdot Bs\left(\theta = \frac{k2\pi}{N}, t\right)$$

Using the definition Torque = Force times moment-arm R, we have

$$Tc[k,t] = R \cdot L \cdot Ic[k,t] \cdot Bs\left(\theta = \frac{k2\pi}{N}, t\right)$$

where

Tc[k] is the torque on the kth conductor, R is the radius

Summing up the contributions of all the N conductors, we have

$$Tc = \sum_{k=1}^{N} R \cdot L \cdot Ic[k,t] \cdot Bs\left(\theta = \frac{k2\pi}{N}, t\right)$$

Where

Tc is the total force on all the conductors.

Under the assumption of large N, we can replace Ic[k] with our continuous approximation λc(θ) and change the sum to an integral.

$$Tc = \int_{s=0}^{2\pi R} R \cdot L \cdot \lambda c(\theta, t) \cdot Bs(\theta st) ds$$

Substitute in our expressions for λc(θ,t) and Bs(θ,t):

$$Tc = \int_{s=0}^{2\pi R} R \cdot L \cdot \lambda\text{max} \cdot \cos(p \cdot \theta - \alpha - w \cdot t) \cdot Bs_{max} \cdot \cos(p \cdot \theta - w \cdot t) ds$$

Pull outside of the integral those items which don't vary with s or $\theta(s)$

$$Tc = R \cdot L \cdot \lambda max \cdot Bs_{max} \int_{s=0}^{2\pi R} cos(p \cdot \theta - \alpha - w \cdot t) \cdot cos(p \cdot \theta - w \cdot t) ds$$

Simplify the integrand using the trig identity $cos(a)cos(b) = 0.5 \cdot [cos(a+b)+cos(a-b)]$
(where $a = p\theta - \alpha - w \cdot t$ and $b = p \theta - w \cdot t$)

$$Tc = R \cdot L \cdot \lambda_{max} \cdot Bs_{max} \cdot 0.5 \cdot \int_{s=0}^{2\pi \cdot R} [cos(2 \cdot p \cdot \theta - \alpha - 2 \cdot w \cdot t) + cos(\alpha)] ds$$

Apply a change of integration variables using $\theta = s/R$, $Rd\theta = ds$

$$Tc = R^2 \cdot L \cdot \lambda max \cdot Bs_{max} \cdot 0.5 \cdot \int_{\theta=0}^{2\pi} [cos(2 \cdot p \cdot \theta - \alpha - 2 \cdot w \cdot t) + cos(\alpha)] d\theta$$

We can now easily see that the first term in the above integral integrates to 0 over this interval (since the integral of a sinusoid in theta over an integral number of periods of theta must be 0), while the second term in the integral is a constant independent of t. Therefore the integral evaluates to:

$$Tc = R^2 L \cdot \lambda max \cdot Bs_{max} \cdot 0.5 \cdot 2\pi \cdot cos(\alpha)$$

(Note again that the time dependence has disappeared, giving a constant total torque on the conductors, even though the individual conductor torques varied with time).

Substitute in our expression for λmax from above gives:

$$Tc = 0.5 \cdot R \cdot L \cdot N \cdot I_{max} \cdot Bs_{max} \cdot cos(\alpha)$$

Replace 0.5 with $1/\sqrt{2} \cdot 1/\sqrt{2}$ gives:

$$Tc = R \cdot L \cdot N \cdot \frac{I_{max}}{\sqrt{2}} \cdot \frac{Bs_{max}}{\sqrt{2}} cos(\alpha)$$

Replace $(max/\sqrt{2})$ with rms values:

$$Tc = R \cdot L \cdot N \cdot I \cdot Bslot \cdot cos(\alpha)$$

Where
  I is rms current in the conductor ($I = I_{max}/sqrt(2)$)
  Bslot is rms fundamental radial flux ($Bslot = Bs_{max}/\sqrt{2}$)
  $cos(\alpha)$ is the rotor power factor. (α is the electrical angle between flux and current).

Subsection 12.4   Part #2 of 4-part proof: Tmotor = R · N · I · L · Bgap · pf

The proof of Part #2 is simply to take the result of Part #1 for force on the conductors and apply the principle of Point 2 (equivalence of total force for conductor in airgap or slot), which we have know is applicable to our rotary geometry from Subsection 12.2 . So we start by imagining all the rotor conductors directly in the airgap flux and compute the torque on the conductors as $T = R \cdot N \cdot I \cdot L \cdot Bgap \cdot pf$ by proceeding exactly as in the previous section. Then if we mentally move those conductors into the slot, we know the total torque (Tmotor) will remain the same:

Tmotor = R· N ·I· L· Bgap·pf

That is the end of the proof of part #2. The next two subsections will cross-check the results of part #2 with textbook equations and real-world motor data, confirming the result. The fact that we reach the correct answer by combining part #1 of 4 with Point 2 (as evidenced by consistency with other references and application to real motor data) also tends to confirm part #1 of 4 and Point 2.

12.4.1   Cross-check of part #2 by calculation with example motor data

Motor Data:
    Squirrel cage induction motor
    11 KW (15 hp)
    6-pole machine
    Pf = 0.85, Efficiency = 0.90 (approx)
    Stator data:
        220V, 3-phase, 60hz power
        Full Load Amps = 39.3
        Airgap diameter = Dgap = 0.24 m
        2-circuit wye
        54 slots
        Stator Slot Height = 0.027 m (~1")
    Rotor data:
        Rotor bar height = 0.016 m (~0.6")
    Other data:
        Airgap depth = g = 0.55E-3 m   (~0.022")
        Ideal stack length = Li = 0.107 m
            (above length doesn't include vent passages or core insulation which don't contribute
            to torque-producing field)
        Peak Airgap Flux Density = 0.66 T

Calculation of torque on this motor at full load using Tmotor=R·N·L·I·Bgap·pf.:

Use the stator side conductor since the stator current is known (*)
R = 0.24 m / 2 = 0.12 m
N = 54 slots · (18 turns/slot) = 972 turns
Li = 0.107 · m
I = 39.3A / 2 = 19.65A (we use half the FLA since this is a 2-circuit wye configuration having two parallel branches, so only half the current flows in each branch).
Bgap = 0.66T / (sqrt(2)) = 0.467 T rms
P.F. ~ 0.85

Find calculated torque (Tcalculated) from equation #2 is as follows:
    Tcalculated = R ·N ·L ·I ·Bgap ·pf. = 0.12 · 972 · 0.107 · 19.65 · 0.467 · 0.85
    Tcalculated = 97.3 Newtons.

Compare this to expected electrical torque (Texpected) based on nameplate data, adjusted for efficiency:
    Texpected = Power / (2 · π · speed · Efficiency)
        Assume 1% full-load slip. Speed ~ 1188 rpm = 19.8 revolutions/second
    Texpected = 11,000 watts / (2 ·Pi · 19.8 hz · 0.9)
    Texpected = 98.2 Newton meter.

Thus we see pretty good agreement between the torque Tcalculated from #2 (Tmotor = R · N · I · L · Bgap · pf) and the torque Texpected that we expect based on the motor nameplate data. We have neglected pitch and distribution factors, and we have not adjusted for the magnetizing current contribution towards full load amps (only the resistive load component of current should be included). Also the power factor and efficiency were not known precisely.

(*) Note that we would expect similar results if this calculation used rotor data, since the amp-turns (N·I) associated with the rotor are equal to those of the stator load component of current.   The same airgap flux density, airgap radius, and active conductor length would apply to rotor and stator.

Conclusion: The full-load torque calculated using Tmotor=R · N · L · I · Bgap · pf matches the nameplate data well.   Similar results would be expected for either the rotor or the stator.

12.4.2   Cross-check of part #2 by comparison to textbook equation.

Reference 9 (Volume 2, page 179) gives the following equation for total torque-producing force:
    F = 6.25E-8 L N Bgap$_{peak}$ Irms p.f. · Kdp
            where F in lbf, L in inches, Bgap$_{max}$ is expressed on peak basis in lines per inch^2.

To facilitate unit analysis, this equation can be interpreted as a product of dimensionless variables, where each variable is divided by the corresponding units to remove the dimensions:

$$\frac{F}{lbf} = (6.25E - 8) * \frac{L}{inch} * N * \frac{Bgap\_peak}{line/in^2} * \frac{Irms}{Amps} * p.f. \cdot Kdp$$

Kdp is a winding factor to account for distributed winding pitch and distribution. This is a unitless factor approx 0.9 for typical motors. This paper does not address the full complexities of a distributed winding and this factor will be neglected (assumed approximately 1.0) in the analysis below.

Now we multiply the right hand side of the above equation by the following bracketed quantities which are each equal to unity:

$$\left[\frac{40 \cdot inch}{meter}\right] \cdot \left[\frac{\sqrt{2} \cdot Bgap\_rms}{Bgap\_peak}\right] \cdot \left[\frac{2.54^2 \wedge 2 \cdot line/in^2}{Gauss}\right] \cdot \left[\frac{10^4 \cdot Gauss}{Tesla}\right] \cdot \left[\frac{4.5 \cdot Newton}{lbf}\right]$$

Then canceling units from top and bottom of right hand side, canceling lbf from bottom of both sides, and dividing both sides by Newtons gives

$$\frac{F}{Newton} = 1 \cdot \frac{L}{meter} \cdot N \cdot \frac{Bgap\_rms}{Tesla} \cdot \frac{Irms}{Amps} \cdot p.f.$$

Now multiplying by R to convert F to T gives:
    Tmotor = R L N Bgap · I · pf (#2)
    Where T is in newton-meters, R and L are in meters, B is in Tesla, I is in amps, and B and I are rms.

Thus our Part #2 expression for total motor torque is equivalent to the equation in Reference 9.

12.4.3   Other references which suggest the same approach
Reference 8 includes the following passage:
    *"It has long been the practice in electrical engineering to approximate the torque of electric machines by the sum of current-field interaction produced by the **total current in each slot and the average flux density in the airgap adjacent to this slot**: T=Sum(i-1..M of: Bnavi *Ii * L * r). Here*

Bn_av_i is the average normal flux density in the airgap corresponding to the ith slot, Ii is the total instantaneous current in the slot, and M is the number of stator slots. Computational tests show that Bnav should be taken over one slot pitch in the airgap under each slot in which the current carrying conductors are located."

The author is suggesting to calculate machine torque by summing together computations of forces which would be generated if the conductors were exposed to the airgap flux density. This is exactly the approach we are taking in our part #2 of 4.

Additionally, references 21, 25, 26, and 27 (excerpts included in Section 22) all support point 2 which is the basis for the approach we have used of calculating total force by substituting a flux density of Bgap into a force on conductor equation.

Subsection 12.5   Part #3 of 4-part proof: Bslot << Bgap

This was addressed in detail in Section 11 . Additionally, note that finite element solutions of motors presented by numerous authors all confirm that Bslot << Bgap. References that support this conclusion include references 10, 11, 12, 13, 14, 15, 16, 18 19, 20, and 27 (relevant excerpts are included in Section 22 at the end of this article).

Subsection 12.6   Part #4 of 4-part proof – the conclusion.

Part #4 combines Parts #1, #2, #3 to show that Tconductor<<Tmotor, and therefore the majority of the total torque-producing force applies not on the conductor but on the core. This may be obvious, but in case it is not:

   #1/#2 = Tconductor/Tmotor = (R·N·L·I·Bslot·pf)/ (R·N·L·I·Bgap·pf) = Bslot/Bgap
   Tconductor/Tmotor = Bslot/Bgap
   If Bslot<<Bgap (#3), then Tconductor<<Tmotor

The bulk of the total torque-producing force does not act on the conductor, and therefore must act on the iron.

Section 13 Graphical Illustration That Force Acts On Iron Slot By Examining Independent Movement Of Conductor And Iron

The four-step proof provides a compelling quantitative proof, but may be missing some intuitive appeal. This section will attempt to provide a more intuitively satisfying graphical illustration that the torque-producing force acts on the iron.

The approach is to use the energy method, and visualize what happens to the flux pattern (and therefore energy) if we independently move the conductor and the iron by a small amount Δx. This movement causes a change in stored energy ΔW. The energy approach tells us the force is the derivative of the energy with respect to position, which can be estimated as F=ΔW/Δx. But it would be difficult to visualize independent movement if the conductor were tight within the slot (as the case of normal electric machines). So we will imagine that the conductor has side clearance within the slot as shown in Figure 14.

Figure 14 (a) /(b) shows the flux pattern of the conductor and slot in their "original position". Figure 14 (c)/(d) shows the conductor moved left. Figure 14 (e)/(f) shows the core moved left.

The figures with the conductor moved left show almost no change in flux pattern. The only noticeable change is within the slot in the very low flux density area that has negligible energy density (remember that

energy density is proportional to flux density **squared**, so a factor of 10 change in flux density equates to a factor of 100 change in energy density). So we conclude that for the conductor

$$F_{conductor} = dW/dx_{conductor} \sim 0$$

In contrast, the figures with the iron slot moved left show a significant change in the high-energy density area of the airgap. The entire airgap flux pattern slides to the left as the iron slides to the left. Thus the high-energy density airgap region on the right-side grows by length Δx_{Iron} and the lower energy density airgap region on the left side decreases by length Δx_{Iron}.   Equivalently, we have moved a volume of airgap $\Delta V = \Delta x_{Iron} \cdot g \cdot L$ from the low-energy left side of the airgap to the high-energy right side of the airgap. Using notation similar to Section 9 , we can compute the change in energy ΔW as follows:

$$\Delta W = \Delta V \cdot (w_{right} - w_{left})$$

where:

$$w_{right} = \frac{B_{right}^2}{2 \cdot \mu_0} \; ; \quad w_{left} = \frac{B_{left}^2}{2 \cdot \mu_0}$$

$$B_{right} = B1 + b2; \; B_{left} = B1 - b2$$

$$b2 = \mu0 \cdot i2/(2 \cdot g)$$

Plugging these values into $\Delta W = \Delta V \cdot (w_{right} - w_{left})$

$$\Delta W = \Delta V \cdot (w_{right} - w_{left}) \;\; = \frac{\Delta V}{2 \mu_0} \cdot (B_{right}^2 - B_{left}^2)$$

$$\Delta W = \frac{\Delta V}{2 \mu_0} \cdot [(B1+b2)^2 - (B1-b2)^2]$$

$$\Delta W = \frac{\Delta V}{2 \mu_0} \cdot [(B1^2 + 2 \cdot B1 \cdot b2 + b2^2) - (B1^2 - 2 \cdot B1 \cdot b2 + b2^2)]$$

$$\Delta W = \frac{\Delta V}{2 \mu_0} \cdot [4 \cdot B1 \cdot b2]$$

$$\Delta W = \frac{\Delta V}{\mu_0} \cdot 2 \cdot B1 \cdot b2$$

Substitute $\Delta V = (\Delta x_{Iron} \cdot g \cdot L)$

$$\Delta W = (\Delta x_{Iron} \cdot g \cdot L) \cdot \frac{2 \cdot B1}{\mu_0} b2$$

Substitute $b2 = \left(\frac{\mu_0 \cdot i2}{2 \cdot g} \right)$

$$\Delta W = (\Delta x_{Iron} \cdot g \cdot L) \cdot \frac{2 \cdot B1}{\mu_0} \cdot \left(\frac{\mu_0 \cdot i2}{2 \cdot g} \right) = \Delta x_{Iron} \cdot L \cdot i2 \cdot B1$$

$$F_{Iron} = \frac{\Delta W}{\Delta x_{Iron}} = L \cdot i2 \cdot B1$$

Figure 14 – Effect of moving conductor or slot

	Flux line plot	Radial airgap flux magnitude plot
Original positions	(a)	(b)
Conductor moved left	(c)	(d)
slot in iron moved left	(e)	(f)
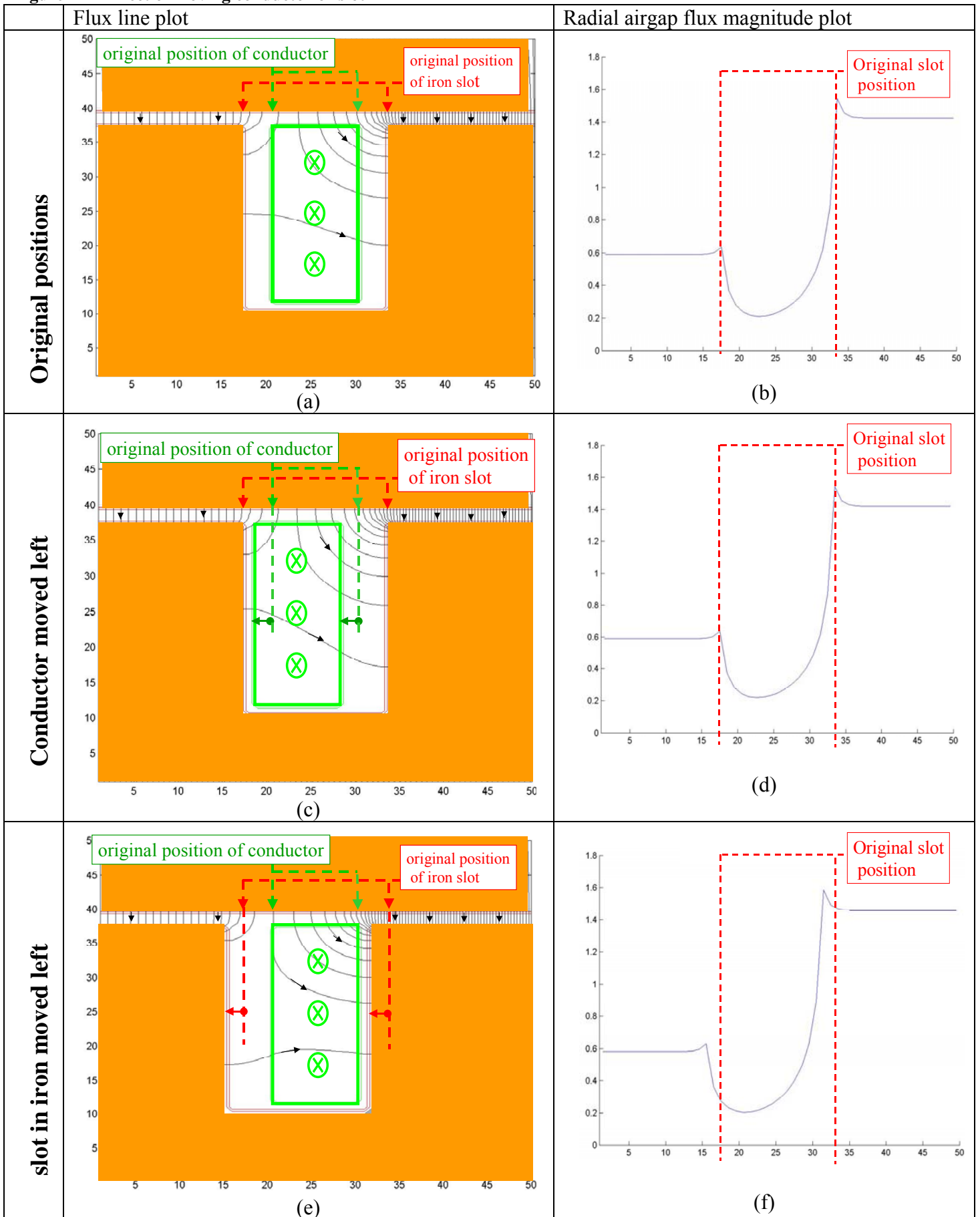
Thus for this geometry ("loose" conductor within slot), by independently moving the conductor and the iron slot a small distance Δx, we have again reached the conclusion that the force on the conductor is close to 0 and the force on the iron is approximately the same as the conductor would have experienced if it were in the airgap flux. The advantage of the approach used in this section is that we can **visualize** the effect on the flux caused by independently moving the conductor or the slot. We see that the high-energy density airgap flux distribution only changes when the iron slot moves (it does not change when the conductor moves).   The substantial change in energy (ΔW) occurs only for movement of the iron slot. **Therefore the force (F=ΔW/Δx) appears primarily on the iron slot.**

Please note that we could have easily reached the same conclusions without any finite element analysis if we can recognize that moving the slot changes the airgap flux density while moving the conductor does not significantly change the airgap flux density. This can be seen as follows.   The only "low-resistance" path for flux is accross the airgap. When we move the slot, we change the location of this low resistance path and we change the energy stored in the airgap on each side of the slot (which results in force on iron shown above). In contrast, if we move the conductor around within the slot, we do not change the location of the low-resistance path and furthermore we do not change mmf accross that low-resistance path accross the airgap (if we draw a loop in iron around the slot crossing the airgap once on each side of the slot, we still have mmf2=i2 around that loop, and we still have airgap flux density b2 = μ0· i2/ [2·g] due to the current within the slot **<u>regardless</u>** of the location of the current within the slot). So we do not change the airgap flux density significantly when we move the conductor and as a result we do not change the energy significantly and we expect very little force on the conductor.

Section 14 Analysis Of Simple Pair Of Conductor Loops By Circuit Energy Approach

We will now introduce the circuit energy approach by going back and analyzing the same geometry that we have previously analyzed with the field energy approach: the simple pair of conductor loops that were previously analyzed and will re-analyze with the circuit approach (Figure 15).   In our analysis we will consider the loop 1 produces the flux density B1 and loop 2 carries the current i2 that will interact with the flux to produce the Lorentz force F=qV**x**B = L i2 **x** B.

Figure 15 - Simple Pair of Conductor Loops (sideview)
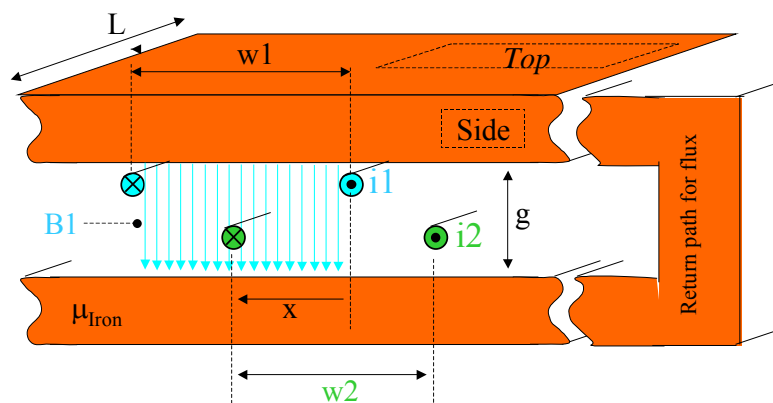
The symbols used in Figure 15 are as follows:
    g - gap dimension
    L - length of conductor within the flux (depth of core into the paper)

w1 - width of loop 1

w2 – width of loop 2

i1 - this is the current in loop 1. We will use i1 to create the flux B1. We will consider i1 to be a purely stationary flux-producing coil... we are not interested in the force on i1.

i2 - this is the current in loop 2.   Loop 2 is the current upon which we will examine the electromagnetic force. The force occurs due to interaction of current i2 and flux density B1. We will determine this force by examining the derivative of energy with respect to position of loop 2.

x - position of loop 2 (compared to loop 1) as shown on the figure. A change in x would correspond to movement of the entire loop 2 (both legs) as if it were a rigid coil.

Bgap - airgap flux density created by current i1 (in the area above/below loop 1)

Φ_{11} - flux from current i1 "linking" loop 1   (See Note [7])

Φ_{21} - flux from current i2 linking loop 1

Φ_{12} - flux from current i1 linking loop 2

Φ_{22} - flux from current i2 linking loop 2

Φ_1 - total flux linking loop 1

Φ_2 - total flux linking loop 2

$\Phi_1 = \Phi_{11} + \Phi_{21} = L1 \cdot i1 + M \cdot i2$

$\Phi_2 = \Phi_{12} + \Phi_{22} = M \cdot i1 + L2 \cdot i2$

L1 = self-inductance of loop 1 (L1= Φ_{11} / i1)

L2 = self-inductance of loop 2 (L2= Φ_{22} / i2)

M = mutual inductance of loops 1 and 2 (M = Φ_{21} / i2 = Φ_{12} / i1)

$\mathcal{R}_{11}, \mathcal{R}_{22}, \mathcal{R}_{12}$ - Reluctances associated with $\Phi_{11}, \Phi_{22}, \Phi_{12}$

We make the same assumptions as before:

> ASSUME that permeability in the iron is very large. i.e. $\mu \gg \mu_0$
>
> ASSUME: g very small. i.e. g $\ll$ w1, w2, L

Again the above two assumptions allow us to focus only on the vertical flux within the airgap and neglect fringing and horizontal flux components. This makes calculation of the circuit parameters L1, L2 and M a trivial exercise in magnetic circuits.   We accomplish the calculation using the magnetic analogy to ohm's law. (Remember the electrical Ohm's law is I = V/R.) The magnetic analogy to Ohm's law is as follows: $\Phi = (N \cdot I)/\mathcal{R}$ where Φ is flux, I is the current that creates the flux, N is number of turns of current (1 in our case), and $\mathcal{R}$ is reluctance. Reluctance is found by $\mathcal{R} = d/(\mu_0 \cdot A)$ where d is the distance that the flux travels in air and A is the area (perpendicular to d) through which the flux travels.

Find L1:

> $\mathcal{R}_{11} = g/(\mu_0 \cdot L \cdot w1)$
>
> $\Phi_{11} = i1 /\mathcal{R}_{11} = i1 \cdot \mu_0 \ L \ w1 \ / \ g$
>
> $L1 = \Phi_{11} / i1 = \mu_0 \ L \ w1 \ / \ g$

Find L2:

> $\mathcal{R}_{22} = g/(\mu_0 \ L \ w2)$
>
> $\Phi_{22} = i2 /\mathcal{R}_{22} = i2 \cdot \mu_0 \ L \ w2 \ / \ g$
>
> $L2 = \Phi_{22} / i2 = \mu_0 \ L \ w2 \ / \ g$

Find M:

> Note that there are two different ways to find M. Both must give the same result by conservation of energy. We choose the second definition which will be easier to work with (M = Φ_{12} / i1)
>
> $\mathcal{R}_{12} = g / (\mu_0 \ L \ x)$

---

[7] flux that "links" a conductor loop flows through the interior of that loop

$$\Phi_{12} = i1 / \mathcal{R}_{12} = i1 \cdot \mu_0 \ L \ x / g$$
$$M = \Phi_{12} / i1 = \mu_0 \ L \ x / g$$

Find Bgap:
$$Bgap = \Phi_{11}/A = i1 \cdot L1/A = i1 \cdot (\mu_0 \ L \ w1 / g) / (L \cdot w1) = i1 \cdot \mu_0 / g$$

The energy in the magnetic field is given by:
$$Wmag = \frac{L1 \cdot i1^2}{2} + M(x) \cdot i1 \cdot i2 + \frac{L2 \cdot i2^2}{2}$$

where we have emphasized the dependence of M upon x.

Using Equation 3, we have:
$$F = \frac{dW}{dx} = i1 \cdot i2 \cdot \frac{d}{dx} M(x) \quad \text{(since L1 and L2 are not functions of x and i1, i2 held constant)}$$
$$F = i1 \cdot i2 \cdot \frac{d}{dx}(\mu_0 \ L \ x / g)$$
$$F = i1 \cdot i2 \cdot \mu_0 \ L \ / g = i2 \cdot L \cdot (i1 \cdot \mu_0 / g)$$

Recognizing the quantity in parentheses as $B1 = i1 \cdot \mu_0 / g$, we can also write
$$F = i1 \cdot i2 \cdot \mu_0 \cdot L \ / g = i2 \cdot L \cdot B1$$
$$F = i2 \cdot L \cdot B1$$

Thus using circuit energy arguments, we have recreated the Lorentz force law $F = qVxB = N \ L \ I \ x \ B$ where in this case there was only one turn (N=1), and B1 played the role of B, and i2 played the role of I. This should give us some confidence in this approach and also reinforce our previous conclusions. We will now proceed to apply the same approach to other geometries of more interest.

Section 15 Analysis Of Shield Tube Configuration By Circuit Energy Approach

Figure 16 - Shield Tube configuration (sideview)
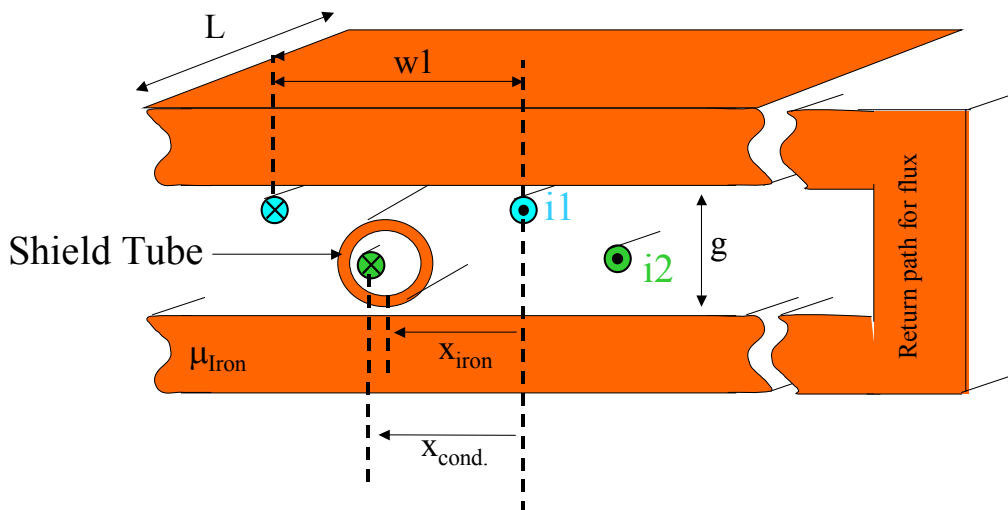
The geometry of the shield tube is shown in Figure 16. It is the same as the previous Figure 15, except that we have added a highly-permeable hollow iron cylinder ("shield tube") around the left leg of conductor loop i2 (we choose the left leg because it is the one that falls within the flux from loop 1). The shield tube is longer than L and therefore extends beyond the rectangular iron on each end. We will examine the effects of independently moving the conductor loop 2 and the shield tube (subject to the constraint that the conductor remains inside the shield tube). Accordingly, instead of using a single variable x for conductor position as before, we now use two variables:

- x_{iron} - position of the center of the iron shield tube
- $x_{conductor}$ - position of the center of the conductor.

As before, we will consider that the self inductances L1 and L2 to remain independent of the position. (This is not strictly true, since L2 will change slightly as we move conductor off-center within the shield, but any variation in L2 as a function of relative position will be related only to the small attractive equal/opposite force pair on the conductor and the shield which represents a net 0 force on the conductor/shield system and is not of interest for this discussion). The parameter of interest remains M which reflects the interaction of the fields from currents 1 and 2.

Figure 17 – illustration of flux from conductor 1 linked to conductor 2
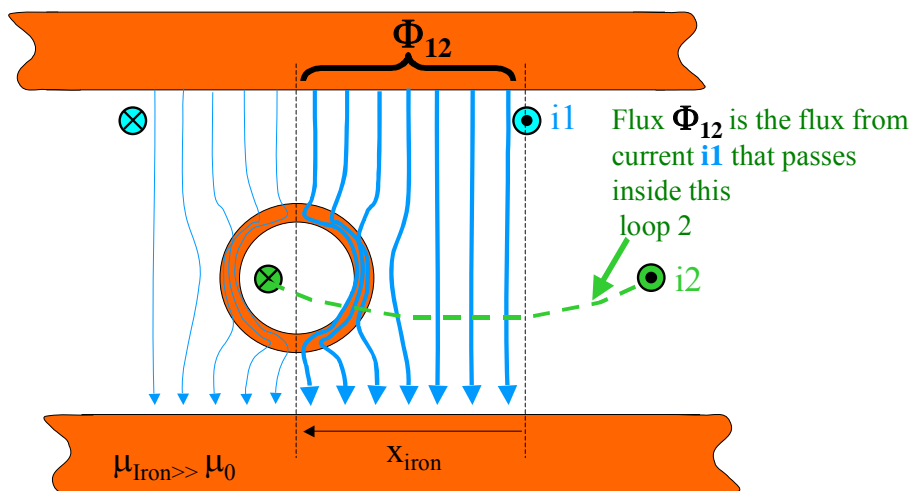
We want to know whether M will depend on x_{iron} or $x_{conductor}$. Again we use the definition $M = \Phi_{12} / i1$. We establish a fixed value of i1 and determine Φ_{12}. Φ_{12} represents the flux from current 1 which is linked by loop 2. We can see from Figure 17 that the flux from current 1 will split at the centerline of the shield tube. All flux to the left of the centerline of the shield tube will flow to the left and will not be linked to current loop 2; all flux to the right of the centerline of the shield tube will flow to the right and will be linked to current loop 2, regardless of the position of current loop 2. Any movement of the conductor loop 2 inside the shield tube (where the flux density from i1 is 0) will not affect how much of the external flux from loop 1 links to loop 2. Therefore M depends directly on x_{Iron} and is completely independent of $x_{conductor}$.

$$\mathcal{R}_{12} = g / (\mu_0 \cdot L \cdot x_{iron})$$
$$\Phi_{12} = i1 / \mathcal{R}_{12} = i1 \cdot \mu_0 \cdot L \cdot x_{iron} / g$$
$$M = \Phi_{12} / i1 = \mu_0 \cdot L \cdot x_{iron} / g$$

Apply Equation 3 using position of conductor to determine force on the conductor:

$$F_{Conductor} = \frac{dW}{dx_{Conductor}} = \frac{d}{dx_{Conductor}}(i1 \cdot i2 \cdot M) = 0, \text{ because the mutual inductance does not depend}$$

on the position of the conductor $x_{conductor}$.

Apply Equation 3 using position of the iron to determine force on the iron:

$$F_{Iron} = \frac{dW}{dx_{Iron}} = i1 \cdot i2 \frac{d}{dx_{Iron}}(M) = i1 \cdot i2 \cdot \frac{d}{dx_{Iron}}(\mu_0 \cdot L \cdot x_{iron} / g)$$

$F_{Iron} = i1 \cdot i2 \cdot (\mu_0 \ L \ / g) = i2 \cdot L \cdot (i1 \cdot \mu_0 / g)$

Remembering that $B1 = i1 \cdot \mu_0 / g$, we can also write

$F_{Iron} = i1 \cdot i2 \cdot \mu_0 \cdot L \ / g = i2 \cdot L \cdot B1$

This is the same result that would be obtained using the Lorentz force equation (Equation 1) for the force on the conductor if it were exposed to the flux density B1. Thus when we added the shield tube outside the conductor, the total force remained the same, but it now acts on the iron shield tube rather than on the conductor!

The shield tube geometry is an idealized geometry which we might intuitively suspect acts very similar to a conductor in an open slot (more later). The advantage of discussing the shield tube geometry lies in the symmetry and simplicity of the behavior which may be easier to visualize than the slot geometry. Additionally, the symmetry of the shield tube allows a complete analytical solution of the magnetic field (not presented here).

Reference 21 provides the complete analytical solution of the magnetic field for this shield tube geometry and applies the Maxwell Stress Tensor method to the solution to determine the forces (a considerably more complex proof than was provided here). The conclusions of Reference 21 are consistent with the conclusions of this paper for the shield tube geometry and rotating machinery in general. Reference 21 provides further discussion of this result and its implications for rotating machinery as indicated in the excerpt in Section 22 .

Section 16 Analysis of Simple Slot Geometry by Circuit Energy Approach

Figure 18 – Conductors in slot
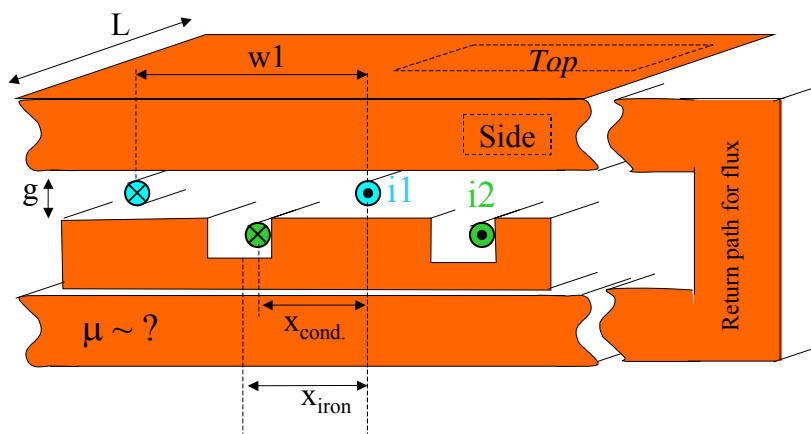
Figure 18 is similar to the shield tube configuration, except we have made it look a little closer to a motor by embedding both of the conductors of loop i2 in a slots within a horizontally-moveable iron piece.   As with the shield tube, we would like to be able to move the conductor and the iron independently. Therefore, we imagine and draw the conductors as if they have side clearance within the slot (similar to Section 13) which will help us visualize independent movement of the copper and the iron.

Again, we will use two variables to describe the position of the iron and conductor:
- x_{iron} - position of the center of the slot that is associated with the left leg of loop i2.
- $x_{conductor}$ - position of the center of the conductor of the left leg of i2

We again consider that the self inductances L1 and L2 are remain independent of the positions.   We again want to know whether M will depend on x_{iron} or $x_{conductor}$.   Again we use the definition $M = \Phi_{12} / i1$.   We establish a fixed value of i1 and determine Φ_{12}. Φ_{12} represents the flux from current 1 which is linked by loop 2.   The relevant figure which shows the patter of flux at the position of a slot (neglecting the contribution from current within the slot is the no-load F.E. solution: Figure 6(a).   From that figure, we see that the flux divides to the left and right based on the centerline of the iron slot (analogous to what we saw in the shield tube configuration).   The only difference is that in this case, a very small amount of the flux enters into the slot area where the conductor is located.   Therefore moving the conductor within the slot would slightly affect Φ_{12}. If we neglect this small amount of flux in the slot, the conclusion is the same as for the shield tube configuration: $M = \Phi_{12} / i1 = \mu_0 \ L \ x_{iron} / g$; $F_{iron} = \ i2 \cdot L \cdot B1$; and $F_{conductor} = 0$.

Qualitatively we can see from this example that the small amount of flux within the slot leads to a weak dependence of M upon Xconductor (as well as the strong dependence on Xiron), which leads to a small force on the conductor.   We can get a feel for the change in force by studying the change in energy as we move the conductor or the iron as shown in Figure 14(c) and Figure 14(e) which show finite element solutions based on moving the conductor and moving the slot by a small amount. We can see that moving the iron to the left has a dramatic effect in increasing the energy stored by increasing the volume of the higher-energy density airgap on the right while decreasing the volume of the lower-energy density airgap on the right. In contrast, movement of the conductor has no noticeable effect on the high-energy density areas of the airgap... and only a small effect on the low energy density areas within the slot.   Knowing that force is determined as change in energy over change in position, this should provide further intuitive confirmation of our conclusion that the force acts primarily on the iron and the solution of the slot problem is very similar to the shield tube problem. (The more rigorous but perhaps less intuitive proof was given in Section 12 .

Section 17 Analysis Of The References

There are some references that say the torque-producing force acts on the conductors (for example references 1, 2, 3, 4 as discussed in Section 4) and some references that say the torque-producing force acts primarily on the iron.   Let us investigate this further.

Subsection 17.1   Why would any textbook say the force acts on the conductors if it's not true?

It gives an easy-to-understand explanation for torque generation, which can be used to correctly predict motor torque.

The force on conductor explanation is simpler and more familiar to most people. It draws on the simple expression for force on the conductor ($F=qV\mathbf{x}B= NL \ I \ \mathbf{x} \ B$) which is taught in high school physics. In contrast, there is no similarly simple, familiar or intuitive expression or explanation for force on iron.

But we can get the correct answer for the total torque producing force by using an equation which looks just like a force on conductor equation (the equation of part #2 of the four-part proof: Tmotor = R· N ·I· L· Bgap· pf) if we simply ignore the selection of B (Bgap vs. Bslot).

So if you are a textbook author and you are want to provide a simple derivation of the torque equation, how do you do it? Just "pretend" that the conductors are in the airgap exposed to a flux density Bslot and use the force on conductor equation! This gives a simple explanation based on familiar principles which gives the correct result and which is intuitively satisfying on a superficial level. It represents a simplification which gives the correct answer for total torque, without accurately representing the nature/location of the torque producing force. As is stated in Reference 21: "*The correct answer is obtained but for the wrong reasons.*" (See excerpt from Reference 21 in Section 22).

Subsection 17.2   How do we know which references to believe regarding where the torque-producing force acts?

With the references providing apparently-conflicting information about whether the torque acts primarily on the core or the conductor, how do we know which references to believe? There is a simple and obvious answer:

> If the reference just mentions that force acts on the conductors without even acknowledging the possibility that there are some forces on BOTH the conductor and the core, and without any basis for distinguishing between force on core and force on conductor, then they have provided no proof and we should suspect they are simply using/repeating the simplification described above for reasons discussed in Subsection 17.1 .

> If the reference acknowledges that there can be force on both the core and conductor and then specifically and deliberately address the theoretical, calculational or experimental basis for distinguishing which has more force, then you know there is no simplification involved and you are going to get a well-considered and well-supported conclusion.

There are 6 references that I believe meet the second criteria of deliberately addressing both possibilities and providing a theoretical, calculational, or experimental basis for drawing a conclusion:
- Reference 22 – Calculates torque-producing force on the stator of permanent magnet motors (conductors within semi-enclosed slots) by finite element analysis. Approx 2% of the force acts on the conductor and 98% on the core.
- Reference 23 - Calculates torque-producing force on the stator of permanent magnet motors (conductors within semi-enclosed slots) by finite element analysis. Concludes that the force on the conductors has "very weak" and does not even tabulate them.
- Reference 24 – Experimental laboratory study determines that force on conductor is 20%-30% of total force (70%-80% acts on core).
- Reference 25 – Concludes that the torque is exerted mainly on the core (vs. conductor) using physical reasoning (similar to the four-part proof).
- Reference 26 – Concludes that the torque is exerted mainly on the core (vs. conductor) using physical reasoning (including analysis using the Maxwell Stress Tensor).
- This paper (Motor Mythbusters... the Long Version) provides the four-part proof that force acts primarily on the core and also provides link to a video demonstration of this principle.

There are a number of additional references that support the conclusion that torque-producing force acts primarily on the core with various lesser degrees of proof:

- Reference 27 – Provides a long discussion supporting the fact that torque-producing force acts primarily on the core, based on the observation that flux takes the path of least resistance which is not through the slot.
- Reference 28 – Provides math analysis of idealized slot configuration leading to his conclusion that torque-producing force acts primarily on the core.
- Reference 29 – States the torque-producing force acts primarily on the core teeth, rather than the conductor.
- Reference 21 – States that the torque-producing force acts primarily on the core (vs. conductor). Provides an analytical proof of this for the idealized shield tube configuration.

Note that excerpts from the above references are available in Section 22 . Additionally references 27, 28, and 29 can be accessed in their entirety on-line using the links shown in Section 22 .

Review of these references will show a pretty sharp contrast. References 1 through 4 indicating force on the conductor simply state that force acts on the conductor **without even mentioning** the possibility that force acts on the core[8], much less providing any proof regarding the relative magnitudes of force on the core or iron. In contrast references 22 through 26 acknowledge and directly address both possibilities and provide a basis (finite element analysis, math analysis, or experiment) for concluding that the majority of the force acts on the core. Also it is noteworthy that references 21 and 26 specifically acknowledge the widespread belief that the torque-producing force acts on the conductor, and yet these references still conclude that force acts primarily on the core. The decision on which references to believe should not be a difficult one.

Section 18 Radial Force On Conductors (Proof Of Point 3)

Point 3 states: "The electromagnetic force that does act on the conductors in slots while under load is primarily in the radial direction, rather than the tangential (torque-producing) direction."

This fact is also not widely known.   Some of the same people that claim the entire torque-producing force acts on the conductor deny the existence of radial electromagnetic forces on the conductors.

Fortunately, Point 3 is the easiest conclusion of all to prove. All we need to do is apply the right-hand rule for direction of force on a conductor (rule was shown in Figure 3.)

Look at Figure 6(e) for an example. The current is into the page. The flux in the slot section (when under load) is primarily in the tangential direction (actually flowing to the right by the right-hand-rule for direction of flux from current).   If we arrange our right hand pointer finger in the direction of the current (into the page) and our right hand center-finger in the direction of the flux (to the right), then our thumb points in the direction of the force (downward, corresponds to the radial direction).

In all motors we know that the current will flow in the axial direction. Further, in all motors with conductors in slots, the flux in the slot section while under load will flow in the tangential direction as shown in references 10, 11, 12, 13, 15, 16, 17, 18, 19, and 20.   The right hand rule for force on conductors will always give a radial force when we have an axial current and tangential flux.

---

[8] Reference 30 is the only reference I have ever seen that addresses the possibility of torque-producing force on iron or conductor and yet still concludes that the force acts primarily on the conductor. The errors in logic are apparent. The author supports the torque on conductor theory using only descriptions of simple devices whose conductors are not located in iron slots. He discounts the force on core on the basis of his assertion that magnetic force cannot act in the torque-producing direction on a laminated iron core (an assertion which is easily disproved by simple experiment with permanent magnet and laminated core).

Additionally, while there are two radial direction (deeper into the slot and out of the slot), the direction of the radial force is always in a direction to move the conductor deeper into the slot. To see this, note that if we reversed the current in Figure 6(e), we would also reverse the direction of the leakage flux and the direction of the force would still be down.   While the direction of the force is always primarily downward, it varies in time, which gives rise to vibration as discussed further in Section 19 .

We have assumed the conductors within a slot are all connected to the same phase and neglect smaller inter-conductor forces (which sum to 0) and considered only the total force. The situation can become more complex if there are coil legs from two different phases in the same stator slot.

The conclusion that the direction of the electromagnetic force acting on current carrying conductors in slots within machines under load is primarily radial (Point 3) is supported by the following references:
- Reference 31 – Provides finite element analysis demonstrating the force on the bars of a squirrel cage motor under load is primarily radial.
- Reference 32 – Provides experimental evidence demonstrating the force on turbine generator stator Roebel bars is primarily radial.
- Reference 33, Reference 34, Reference 35 - Provide similar discussion.

Excerpts of these references are included in Section 22 .

Section 19 Example Examination Of a Coils

We may be faced with the task of examining failed coils to determine the cause of failure. We would like to be able to determine the forces that have acted on the cores by inspection.   Below is a form-wound individual-coil vacuum pressure impregnated coil. The coil sides show distinct lines indicating radial movement against the core.   The pattern of those lines is interrupted at each vent duct opening, where no wear occurs and we can still easily see the original weave of the armor tape (on the bottom of the coil, we also see the original weave of the iron tape).   Some people call this pattern on the side a "ladder pattern" for obvious reasons.   It shows that the coil was loose within the slot and that the loose coil was acted upon by the expected time-varying radial force during operation.

Figure 19 – Example of loose abraded coil

The conclusions that can be drawn from post-mortem examination of this type of coil involve some degree of judgment and subjectivity. I don't make any claim that we can completely determine all of the forces by examining the coil. But to give ourselves the best chance to reach the correct conclusion when examining coils, we need to start with the best understanding of the expected forces within the motor. This is not served by the myth that the entire motor torque acts directly upon the conductor.

Section 20 Conclusion:

The four-part proof of Section 11 and Section 12 is very straightforward and deals with the fundamental quantities of Tconductor (torque acting on the conductors) and Tmotor (total torque acting in the motor). The torque-producing force on the conductors can be computed from a simple formula derived from the Lorentz force equation, which includes the radial flux density at the location of the conductors: Bslot.   By careful consideration of Point 2 (total force is the same for conductor in slot or airgap), we saw that the total torque-producing force of the motor is the same simple formula, but includes a factor of Bgap (radial airgap flux density) instead of Bslot. Since Bslot is much less than Bgap, it is easily seen that the torque producing force on the conductors must be much less than the total torque-producing force.   Therefore, the majority of the torque producing force must act on the core, rather than the conductors.

We should not attach an undue significance to comments from a few references (for example reference 1-4) that imply that the torque-producing force acts solely on the conductors, without even mentioning possibility that the force acts on the iron, much less providing any proof of where the force acts.   There is an obvious motivation to use this simplification since it is easier to explain/understand (F=qVxB is easier than the energy approach or Maxwell stress tensor) and gives a shortcut for deriving the correct expression for total torque if we ignore/gloss-over the choice of flux density B (Subsection 17.1).

In contrast, there is no shortage of references that specifically and directly address the question of torque on the conductor vs. torque on the core (Subsection 17.2).   These references conclude that the force acts primarily on the core when the conductors are located in slots. This is proven in the references by theoretical analysis, by finite element analysis, and by experiment. It is also available to see with your own eyes in video form (Section 5).

Section 21 List of References

1. "Preventive Maintenance of Electrical Equipment", by Hubert, Charles, McGraw-Hill, New York, 1955
2. Wikipedia entry for "electric motor" at   http://en.wikipedia.org/wiki/Electric_motor
3. "Practical Troubleshooting of Electrical Equipment and Control Circuits" by Mark Brown, Jawahar Rawtani, and Dinesh Patil, Newnes/Elsevier ISBN 0-7506-6278-6
4. "Standard Handbook for Electrical Engineers", 13th ed, edited by Fink and Beaty.
5. "Mechanical Vibrations", J. P. Den Hartog, Dover Publications, ISBN 0-486-64785-4 (p. 72)
6. "Electromagnetic Fields and Waves", 3rd Ed. by Lorrain and Corson, ISBN 0-716-71823-5
7. "The Electrical Engineering Handbook", Edited By Wai-Kai Chen ISBN: 0-12-170960-4
8. "Permanent Magnet Synchronous Motor: Finite Element Torque Calculations", Chang, L.   Eastham, A.R.   Dawson, G.E., Dept. of Electr. Eng., Queen's Univ., Kingston, Ont.; Conference Record of the 1989 IEEE Industry Applications Society Annual Meeting, 1989
9. "Electrical Machinery" by Liwshitz-Garik and Whipple, Copyright 1946, Van Nostrand Company
10. "Electromagnetic Modeling By Finite Element Methods", By Bastos and Sadowski, ISBN: 0-8247-4269-9
11. "Handbook Of Electric Motors" by Kilman, Toliyat
12. "Influence of Rotor Slot Wedges on Stator Currents and Stator Vibration Spectrum of Induction Machines: A Transient Finite-Element Analysis" by Koen Delaere, Ronnie Belmans, and Kay Hameyer, IEEE Transactions On Magnetics, Vol. 39, No. 3, May 2003
13. "1150 hp motor design, electromagnetic and thermal analysis", by Qasim Al'Akayshee 1, and David A Staton ", page 5
14. "Force and Vibration Analysis of Induction Motors" by D. Mori and Takeo Ishikawa, IEEE Transactions On Magnetics, Vol. 41, No. 5, May 2005

15. "Detection of Broken Bars in the Cage Rotor on an Induction Machine", by Nagwa M. Elkasabgy, Anthony R. Eastham, and Graham E. Dawson, IEEE Transactions On Industry Applications, Vol. 28, No. 1, January/February 1992

16. "Simulation of the Electromechanical Faults in a Single-Phase Squirrel Cage Induction Motor", by G. H. Jang, Member, IEEE, and S. J. Park, IEEE TRANSACTIONS ON MAGNETICS, VOL. 39, NO. 5, SEPTEMBER 2003

17. "Industrial Power Engineering and Applications Handbook", by K.C. Agrawal. Butterworth-Heineman 2001

18. "Reduction of Electromagnetic Force Harmonics in Asynchronous Traction Motor by Adapting the Rotor Slot Number" by Byung-Taek Kim, Byung-I1 Kwon, IEEE Transactions On Magnetics, Vol 35, No 5. September 1999

19. "Finite Element 2D Steady-State Time Harmonic Field Analysis of Induction Motor" by Ajay Kumar, Sanjay Marwaha, and Anupama Marwaha, IEEE India Annual Conference 2004, Indicon 2004

20. "Numerical Computation Of Torques in Permanent Magnet Motors By Maxwell Stresses And Energy Method", by M. Marinescu And N. Marinescu, IEEE Transactions On Magnetics, Vol. 24, No. 1, January 1988

21. "Electromagnetic Field Theory" by Zahn, ISBN 0-471-02198-9, pages 370-373

22. "Separation of Each Torque Component on Parts of Electric Machine Using Magnetic Force Density" by Hong Soon Choi, Joon Ho Lee and Il Han Park, IEEE TRANSACTIONS ON MAGNETICS, VOL. 41, NO. 5, MAY 2005.   (This is item D1 in discussion of references).

23. "Determination Of Synchronous Motor Vibrations Due To Electromagnetic Force Harmonics" By Y. Lefevre, B. Davat And M. Lajoie-Mazenc, Ieee Transactions On Magnetics, Vol. 25, No. 4, July 1989. (This is item D2 in discussion of references).

24. "Fundamental study on improvement of electromagnetic torque characteristics in electric machines of slot structure", by Ueda, R. Sonoda, T. Ishiguro, M. Furuta, T. Kyushu Inst. of Tech. From Magnetics Conference, 1989. Digests of INTERMAG '89., International Publication Date: 28-31 Mar 1989 On page(s): HP12-HP12   (This is item D6 in discussion of references).

25. "Electric Machines and Drives", by Slemon, ISBN 0-201-57885-9 (page 93)

26. "Induction Machine Handbook", by Boldea, Ion and Nasar, Syed,CRC Press, Boca Raton, FL, 2002

27. "Electric Motors and Drives: Fundamentals, Types, and Applications" By Austin Hughes.

28. On-line electromagnetics course, Chapter 6 - Motor Dynamics by G2 Consulting, George P. Gogue, Ph.D· (http://www.consult-g2.com/course/chapter6/chapter.html)

29. "Finite Element Methods in Electrical Power Engineering" By A.B. J. Reece, T. W. Preston. Published in Electrical Insulation Conference, 1997, and Electrical Manufacturing & Coil Winding Conference Proceedings

30. "Forces on the Rotor Bars of a Three Phase Induction Motor", by Howard W. Penrose

31. "Analysis of the Mechanical Stresses on a Squirrel Cage Induction Motor by the Finite Element Method", by Chang-Hoon Juri and Alain Nicolas, from IEEE TRANSACTIONS ON MAGNETICS, VOL. 35, NO 3, MAY 1999.

32. "Investigation of High Voltage Stator Winding Vibrations in Faul-Scale Slot Model." by Viktor Kogan and Beant Nindra National Electric Coil Company, L.P.

33. "Slot Discharge Mechanisms In High Voltage Rotating Machines" by D G Edwards of The Robert Gordon University, UK

34. "Measures and Technologies to Enhance the Insulation Condition Monitoring of Large Electrical Machines", by J. Keith Nelson and Saber Azizi-Ghannad, IEEE Transactions on Dielectrics and Electrical Insulation Vol. 11, No. 1; February 2004

35. EPRI TR 5036 (Power Plant Electrical Reference Series), Volume 16 ("Handbook to Assess the Insulation Condition of Large Rotating Machines")

36. "Electrical Insulation For Rotating Machines" By Greg Stone, Edward A. Boulter, Ian Culbert, And Hussein Dhirani ISBN 0-471-44506-1

Section 22 Excerpts from References 10 through 36

Excerpt from Reference 10 - "Electromagnetic Modeling By Finite Element Methods",
By Bastos and Sadowski, ISBN: 0-8247-4269-9

Stator core backiron

Airgap
Rotor conductors/bars

Stator Conductors/coils

Rotor core teeth

Rotor core backiron
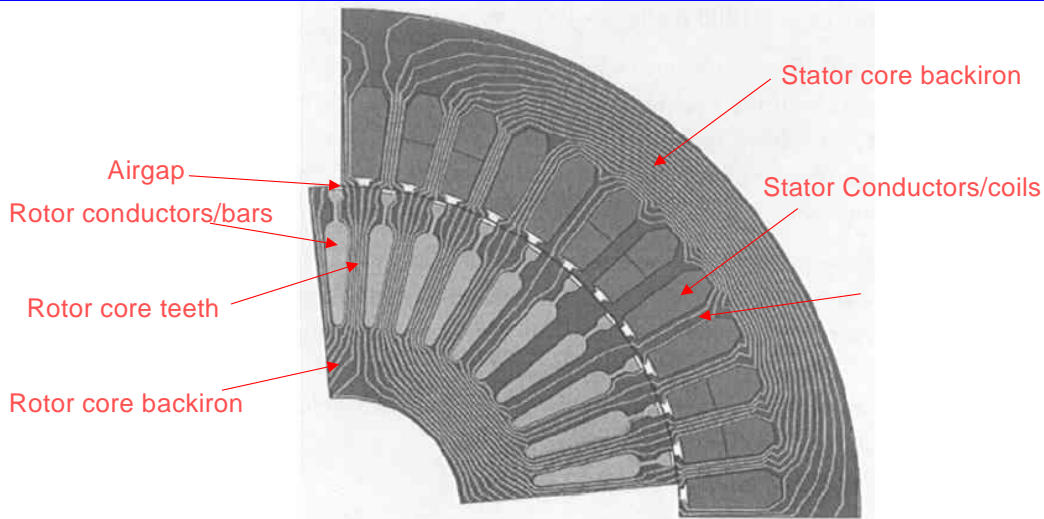
Figure 6.14. Field distribution in the three-phase induction motor.

[This figure is at no-load.]

Note that what little flux
is in the slot is tangential
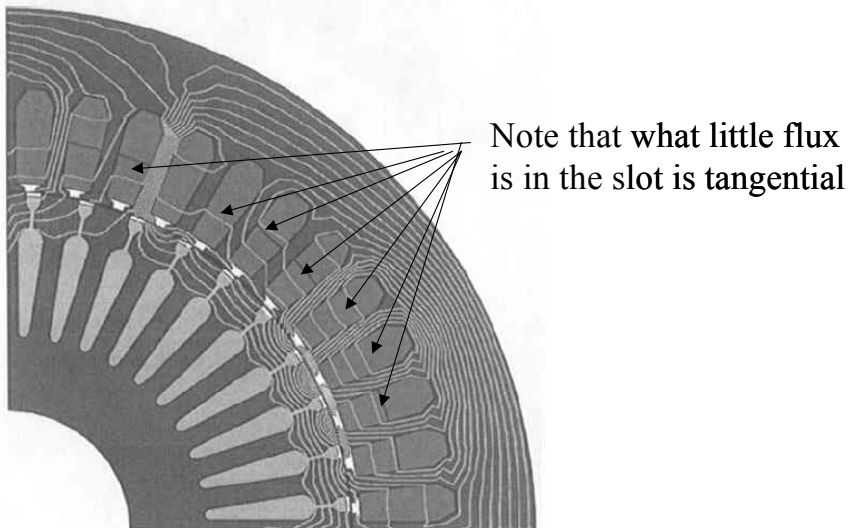
Figure 5.18. Magnetic flux distribution in a four-pole induction motor.

[This figure is at full-load.]

Peter's comments:
- The first figure was at no-load and the second figure was at full load. Both show very low flux in the both the rotor and stator slots where the conductors are since the flux lines are very far apart in the slot. A small tangential flux appears in the stator slot when load is added (the lines travel across the slot in the tangential direction and are still far apart).
- Supports
  - Bslot << Bgap (radial component) (item #3 of four-part proof)
  - Flux in the slot is primarily tangential direction.

End of Excerpt from Reference 10

Excerpt from Reference 11 - "Handbook Of Electric Motors" by Kilman, Toliyat (*)
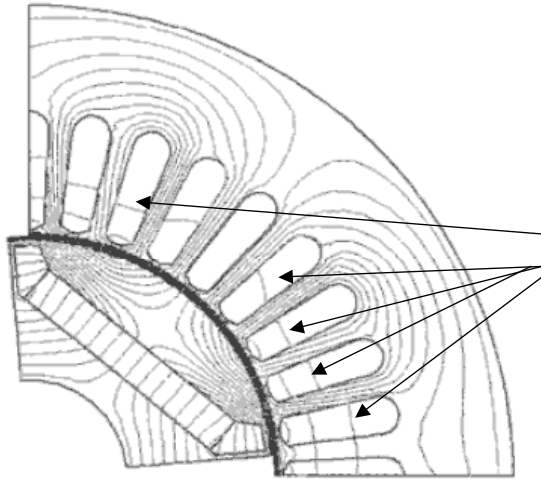
Note that what little flux is in the slot is tangential

Figure 4.100 Finite-element computation of the magnetic field in a permanent-magnet brushless motor with a strongly demagnetizing current in the negative direct axis.

Peter's comments
This is a permanent magnet motor, but the stator is identical to an induction motor.
- Supports
  - Bslot << Bgap (radial component) (item #3 of four-part proof)
  - Flux in the slot is primarily tangential direction.

End of Excerpt from Reference 11

Excerpt from Reference 12 - "Influence of Rotor Slot Wedges on Stator Currents and Stator Vibration Spectrum of Induction Machines: A Transient Finite-Element Analysis" by Koen Delaere, Ronnie Belmans, and Kay Hameyer, IEEE Transactions On Magnetics, Vol. 39, No. 3, May 2003
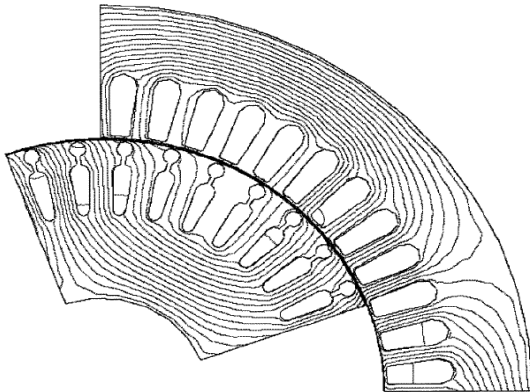
Fig. 1.   Magnetic field inside the induction machine for rotor pos

Peter's comments
- Induction motor under load:
- Supports
  - Bslot << Bgap (radial component) (item #3 of four-part proof)
  - Flux in the slot is primarily tangential direction.

End of Excerpt from Reference 12

Excerpt from Reference 13 - "1150 hp motor design, electromagnetic and thermal
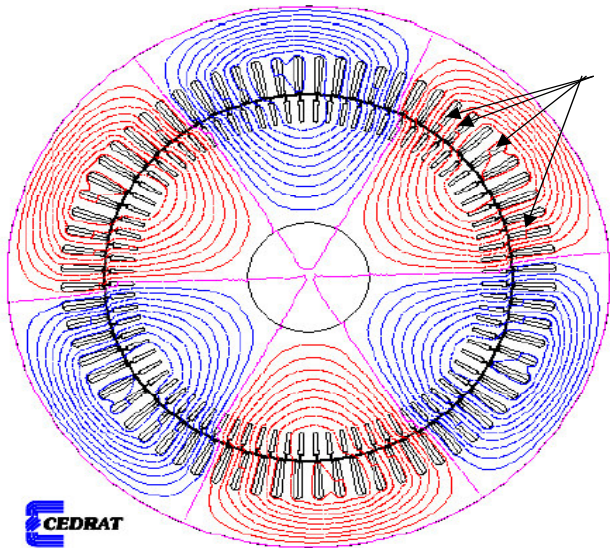
Note that what little flux is in the slot is tangential

Fig.13. FEA flux plot (rated condition)

Peter's comments
- The above is a 1150 HP 6-pole motor at full load.
- Supports
    o Bslot << Bgap (radial component) (item #3 of four-part proof)
    o Flux in the slot is primarily tangential direction.

* Available at http://www.cedrat.com/software/motor-cad/pdf/Motor-CAD_2002.pdf

End of Excerpt from Reference 13

Excerpt from Reference 14 - "Force and Vibration Analysis of Induction Motors" by D. Mori and Takeo Ishikawa, IEEE Transactions On Magnetics, Vol. 41, No. 5, May 2005

θ
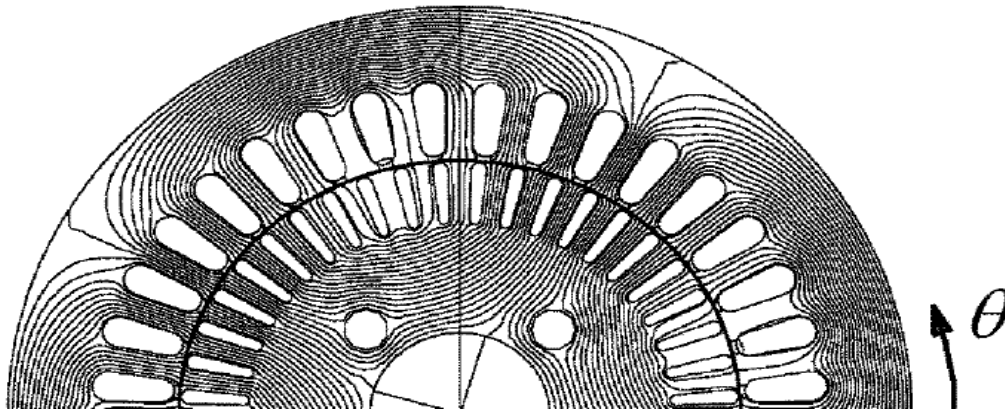
Peter's comments
- Induction motor at no-load.
- Supports
    o Bslot << Bgap (radial component) (item #3 of four-part proof)

End of Excerpt from Reference 14

Excerpt from Reference 15 - "Detection of Broken Bars in the Cage Rotor on an Induction Machine", by Nagwa M. Elkasabgy, Anthony R. Eastham, and Graham E. Dawson, IEEE Transactions On Industry Applications, Vol. 28, No. 1, January/February

1992
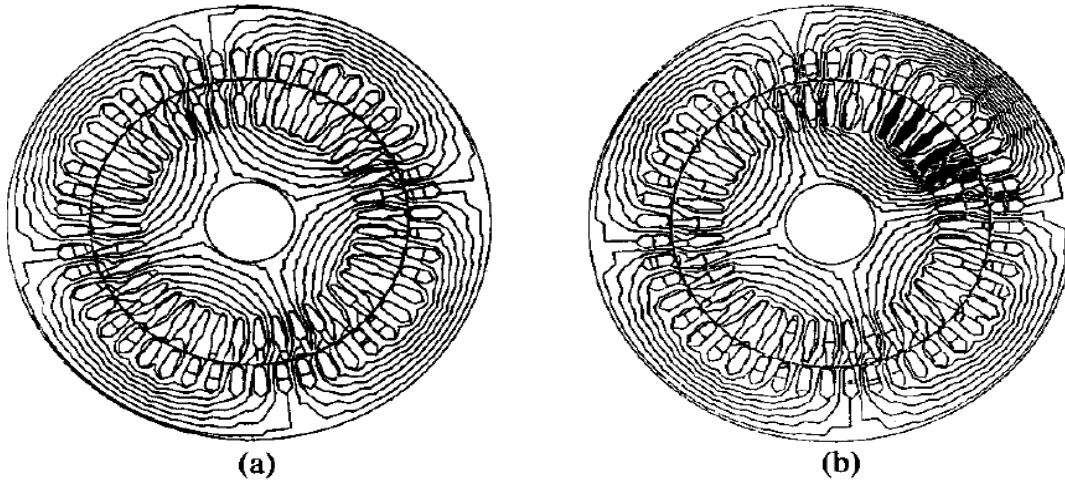
Fig. 2. Field distribution at full load (1760 r/min): (a) No broken bars; (b) five broken bars (shown shaded).

Peter's comments
- Induction motor at full load.
- Supports
  - Bslot << Bgap (radial component) (item #3 of four-part proof)
  - Flux in the slot is primarily tangential.

End of Excerpt from Reference 15

Excerpt from Reference 16 - "Simulation of the Electromechanical Faults in a Single-Phase Squirrel Cage Induction Motor", by G. H. Jang, Member, IEEE, and S. J. Park, IEEE TRANSACTIONS ON MAGNETICS, VOL. 39, NO. 5, SEPTEMBER 2003
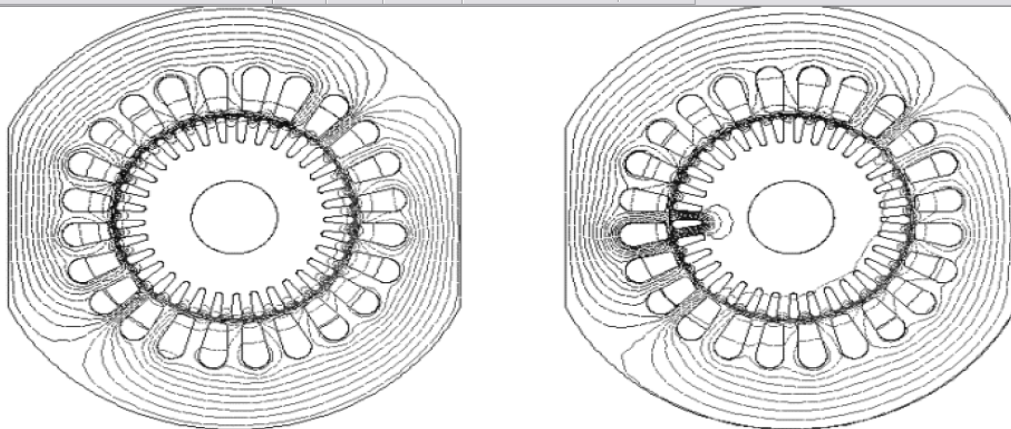
Fig. 3. Magnetic flux distribution in the cases of a normal rotor cage and a broken bar.

Peter's comments:
- Supports
  - Bslot << Bgap (radial component) (item #3 of four-part proof)
  - Flux in the slot is primarily tangential.

End of Excerpt from Reference 16

Excerpt from Reference 17 - "Industrial Power Engineering and Applications

Motor torque, load torque and selection of motors **2/39**
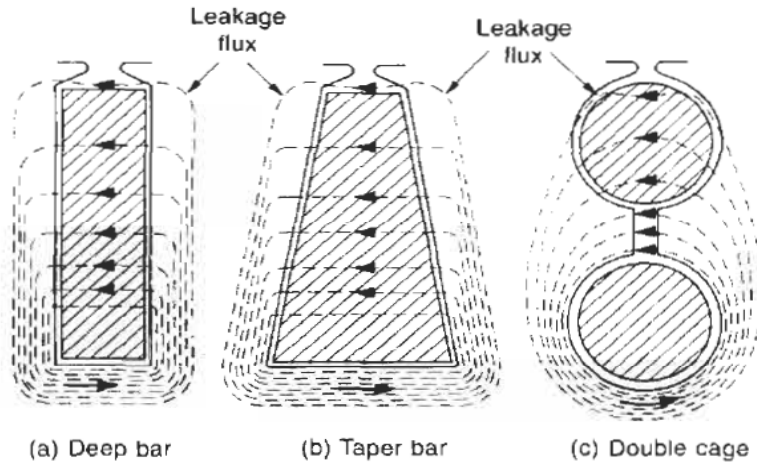
Figure 2.6 Different types of rotor slots, making use of skin effect

Peter's comments
- This shows absolutely no radial component in the slot.
- This shows the tangential cross-slot leakage flux arising from rotor current.
- This looks similar to the pattern for current only shown in Figure 6(c).
- Supports: Flux in the slot is primarily tangential.

End of Excerpt from Reference 17

Excerpt from Reference 18 - "Reduction of Electromagnetic Force Harmonics in Asynchronous Traction Motor by Adapting the Rotor Slot Number" by Byung-Taek Kim, Byung-I1 Kwon, IEEE Transactions On Magnetics, Vol 35, No 5. September 1999
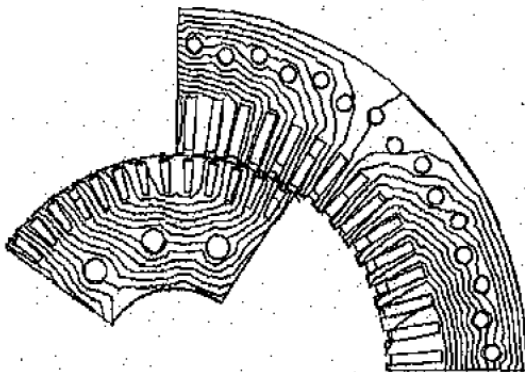
Fig. 2. Flux plot when the rotor slot number is 52

Peter's comments
- An asynchronous traction motor is a type of induction motor.
- Supports
  - Bslot << Bgap (radial component) (item #3 of four-part proof)
  - Flux in the slot is primarily tangential.

End of Excerpt from Reference 18

Excerpt from Reference 19 - "Finite Element 2D Steady-State Time Harmonic Field

Analysis of Induction Motor" by Ajay Kumar, Sanjay Marwaha, and Anupama Marwaha, IEEE India Annual Conference 2004, Indicon 2004
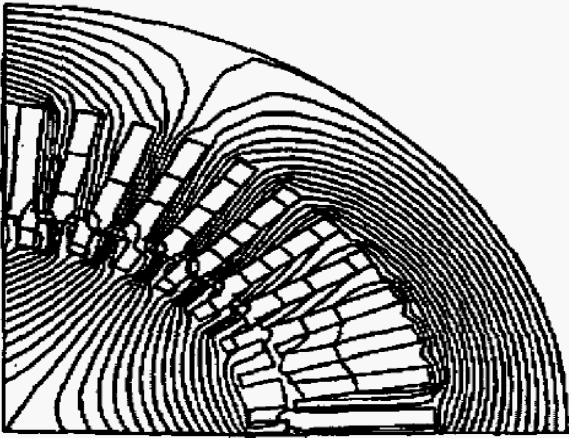
Fig 1: Flux Plot for Induction Motor at t =

Peter's comments:
- Supports
  - Bslot << Bgap (radial component) (item #3 of four-part proof)
  - Flux in the slot is primarily tangential.

End of Excerpt from Reference 19

Excerpt from Reference 20 - "Numerical Computation Of Torques in Permanent Magnet Motors By Maxwell Stresses And Energy Method", by M. Marinescu And N. Marinescu, IEEE Transactions On Magnetics, Vol. 24, No. 1, January 1988

Fig 5 - No-load

Fig 6 - Full-load
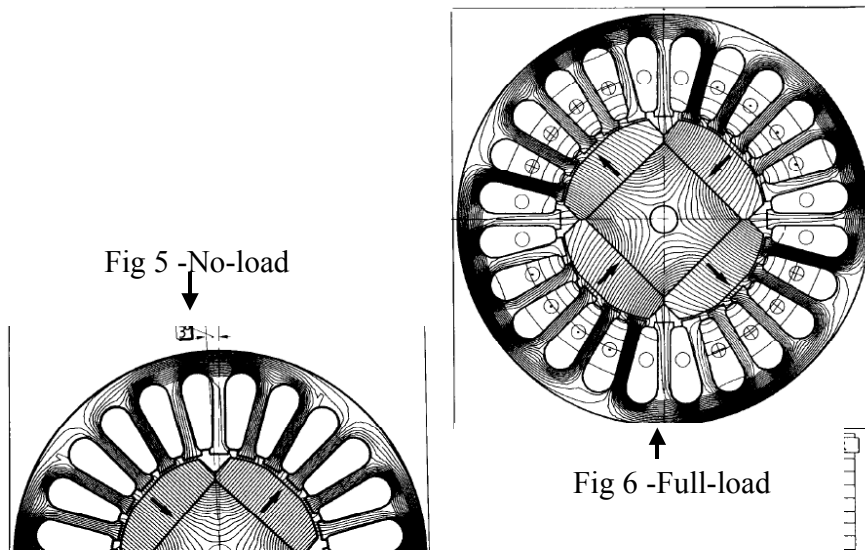
Peter's comments.
- This is a PM motor with stator identical to induction motor.
- Both the no-load and full-load figures show very little flux in the slot. A small tangential component of flux appears in the slot under load.
- Supports
  - o Bslot << Bgap (radial component) (item #3 of four-part proof)

End of Excerpt from Reference 20

Excerpt from Reference 21 - "Electromagnetic Field Theory" by Zahn, ISBN 0-471-02198-9, pages 370-373

"The force on the [iron] cylinder [in the case of infinite permeability] is the same as that of an unshielded current carrying wire, given by F=I*B0*L. If the iron core has a finite permeability, the total force on the wire (Lorentz force) and on the cylinder (magnetization force) is again equal to F=I*B0*L. This fact is used in rotating machinery where current carrying wires are placed in slots surrounded by highly permeable iron material., **Most of the force on the whole assembly is on the iron and not on the wire, so that very little restraining force is necessary to hold the wire in place. The force on a current-carrying wire surrounded by iron is often calculated using only the Lorentz force, neglective the presence of the iron. The correct answer is obtained but for the wrong reasons. Actually there is very little B field near the wire as it is almost surrounded by the high-permeability iron so that the Lorentz force on the wire is very small. The force is actually on the iron core."**

Peter's comments:
- This book includes an analyitical solution of the field for the shield tube geometry (not excerpted here) which supports the conclusions of this paper.
- Supports Point 1 (torque acts primarily on iron vs conductor) and point 2 (total force for conductor/slot is the same as the force that the conductor would experience if it were directly in the flux airgap).

End of Excerpt from Reference 21

Excerpt from Reference 22 - "Separation of Each Torque Component on Parts of Electric Machine Using Magnetic Force Density" by Hong Soon Choi, Joon Ho Lee and Il Han Park, IEEE TRANSACTIONS ON MAGNETICS, VOL. 41, NO. 5, MAY 2005.   (This is item D1 in discussion of references).

"Abstract: For the mechanical structure design of electric machines, each force component on parts of an electric machine need to be separated. In this paper, a separation scheme of each torque component is presented. It is based on the magnetic force density analysis of the general formulation of equivalent magnetic charge method and Lorentz force density. The force density analysis can be applied to all parts of the system region including the inside of material and the interface of different materials. An interior permanent magnet motor and a surface permanent magnet motor are adopted for numerical test in this paper. Their numerical results show validity and usefulness of the presented method....
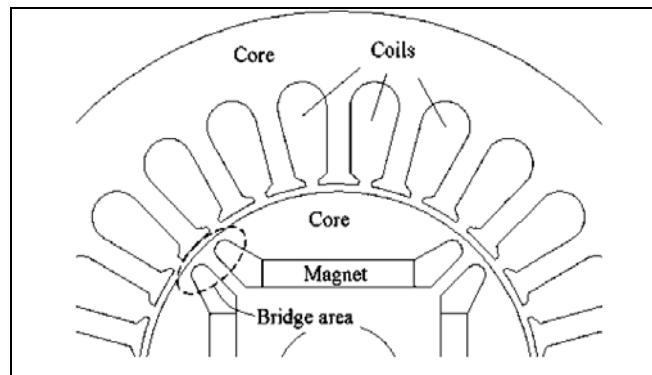
Fig. 2.   Part of IPM motor for torque calculation.
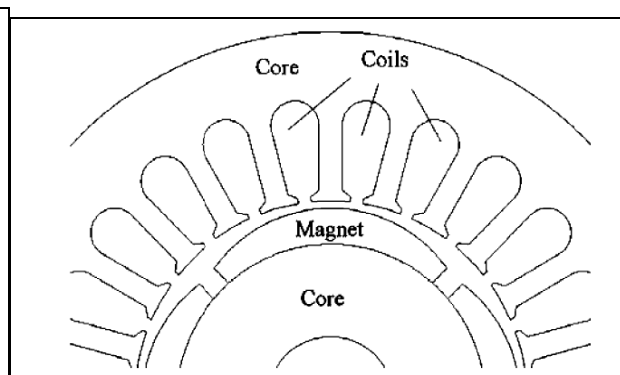
Fig. 6.   Part of SPM motor for torque calculation.

TABLE I TORQUE CALCULATION AT PARTS (UNIT: Nm) OF IPM MOTOR					
Rotor			Total	Stator	
Total	Magnet	Core		Core	Coil
5.19	0.06	5.13	-5.48	-5.42	-0.06

TABLE II TORQUE CALCULATION AT PARTS (UNIT: Nm) OF SPM MOTOR					
Rotor			Total	Stator	
Total	Magnet	Core		Core	Coil
10.03	9.62	0.41	-9.71	-9.57	-0.14

Peter's comments:
- The author performed F.E. analysis of two types of small permanent magnet synchronous motors: Interior Permanent Magnet (IPM) and Exterior Permanent Magnet (EPM). These two types of motors differ only in the configuration of their rotor. We are not interested in the rotors which do not have conductors or slots. We are interested in the stators which as shown in figures 2 and 6 are identical to the stators used in induction motors (for example random-wound motor with semi-closed slots).
- Tables I and II provide the results. Comparing the last two columns of each table which describe the torque on the core and the coil, we see that for both motors (IPM and SPM), about 98% of the torque acts on the core and 2% acts on the coil (conductor).
- <u>Supports</u> Point 1 (torque acts primarily on iron vs conductor).

End of Excerpt from Reference 22

Excerpt from Reference 23 - "Determination Of Synchronous Motor Vibrations Due To Electromagnetic Force Harmonics" By Y. Lefevre, B. Davat And M. Lajoie-Mazenc, Ieee Transactions On Magnetics, Vol. 25, No. 4, July 1989.   (This is item D2 in discussion of references).

"Abstract: In this paper the authors present a method of computation of the magnetic vibrations produced by electric motors. The method is based first on the calculation of the electromagnetic field in the motor. Then the fluctuations of the magnetic forces applied on the teeth of the stator are evaluated. Finally harmonics of these magnetic forces are calculated to lead by means of a mechanical finite element analysis to the motor vibrations. The method is applied to compare vibrations produced by two permanent magnet synchronous motors of different magnetic structures....

...Magnetic forces are applied on the conductors in slots and on the teeth of stators. Magnetic forces exerted on conductors are calculated by the Laplace's law and magnetic forces on teeth are calculated by the Maxwell's stress tensor. In a previous paper the authors showed experimentally that integration of the surface force density given by the Maxwell's stress tensor over a surface covering partially a tooth of a motor leads to magnetic force applied on this tooth. Calculations of forces on conductors and on teeth give a good evaluation of the distribution of the magnetic forces along stators of electric motors....

..Figure 2 and figure 3 show the time evolution of the radial and the tangential magnetic forces applied on the three teeth of a pole of the stator. **Forces on conductors are not shown because they have very weak value.**

Peter's Comments:
- Again we will focus on the stator results which will be comparable to the rotor and stator of an induction motor (conductors in slots).
- The author sets out to calculate forces on both the conductors and iron based on a finite element solution.
- The author calculated both radial and tangential (torque-producing) forces on both

the conductors and the core. The magnitude of the forces on the conductor were not even tabulated because they were much lower magnitude.
- Although the primary interest of this paper is dynamic forces causing vibration, the calculated tangential (torque-producing) force plotted in figures 2 and 3 includes the sum of the dynamic and static (mean) component. This is further demonstrated by the following statement: "the mean values of the tangential forces [on these two PM syncronous motors with different rotors] are equal; this result agrees with the fact that the two motors have the same torque."
- <u>Supports</u> Point 1 (torque acts primarily on iron vs conductor)

End of Excerpt from Reference 23

Excerpt from Reference 24 - "Fundamental study on improvement of electromagnetic torque characteristics in electric machines of slot structure", by Ueda, R. Sonoda, T. Ishiguro, M. Furuta, T. Kyushu Inst. of Tech. From Magnetics Conference, 1989. Digests of INTERMAG '89., International Publication Date: 28-31 Mar 1989 On page(s): HP12-HP12   (This is item D6 in discussion of references).

"... The purpose of this paper is to present a fundamental study for searching the possibility of the improvement. At first, behaviors of the force acting on a conductor placed between the magnetic poles are investigated by using a device shown in Fig.1, where the total system is indicated in Fig.(a) and Fig.(b) shows the geometrical dimension of the magnetic field generator. Fig.2 (a) indicates the measurement point of the magnetic flux density and the measured results are swmnarized in Fig.2 (b)...

...Next, the problem of the force distribution is discussed when the conductor is inserted into a slot. The slot model and the total system under study are indicated in Fig.4 (a) and (b) respectively. The set of five rectangular conductors can be inserted in a slot. The length of each conductor is 250mm. The total cross-sectional area of the conductors is 10mm x 14 mm. The maximum allowable current totally can amount to 1500A for a few seconds. **Then the force Fc acting on the conductors only and the force Fi, acting on the iron part are separately measured** and their results are indicated in Fig.5. The Fi is measured over three times. **The Fc is only 20-30% of the total force.** In this case, the set of the conductor is untouched to the iron surface in the slot. Accordingly, the Fc does not make any contribution as the driving force to the iron part."

Peter's comments:
- The authors use an experimental rig to simulate a current carrying conductor in a slotted core in an electric machine. Their results are that the force on the conductor is 20-30% of the total force and the force directly on the iron is 70%-80% of the total force.
- <u>Supports</u> Point 1 (torque acts primarily on iron vs conductor).

End of Excerpt from Reference 24

Excerpt from Reference 25 - "Electric Machines and Drives", by Slemon, ISBN 0-201-57885-9 (page 93)

"3.4 - *Placing Conductors in Slots*.   The elementary machine of the previous section contained a conducting loop rotating about a cylindrical iron core. To provide greater mechanical rigidity, the conductor could be attached to the surface of the iron core and the combined assembly or rotor could be rotated. This arrangement involves a continually changing flux density in the iron core. To prevent excessive eddy current losses, the core may then have to be made of a stack of circular laminations, as discussed in section 1.8. With this arrangement, the conductor is still in the magnetic field and the

relations of Equations 3.8 and 3.11 apply [F = qVxB = NLIxB].

Let us now consider the possibility of fitting each side of the conductor loop into a slot in the rotor surface , as shown in Figure 3.8(a). This would allow the air gaps between the rotor and outer stationary magnetic system or stator to be made just large enough for mechanical clearance. The same flux density could then be produced in the air gaps with a much lower mmf from the stator.

On first examination, it might appear that the machine would no longer operate as before. **The conductor is now in a region of very low flux density because most of the flux takes the short path across the air gap and little penetrates down into the slot**, as shown in the field plot of Fig 3.8B. [figure 3.8B looks very much like the field solution I provided in   above].   The direct torque on the conductor loop carrying current i will still be given by equation 3.9 [T = 2*R N L I x B], but will be quite small. On the other hand, the flux linkage λ of the loop will still change as the loop is rotated in essentially the same manner as when the conductor was on the surface of the core. Thus the overall torque as given by Equation 3.19 [T = I * dλ/dθ] should be unchanged.

In explanation, the torque is mainly exerted on the iron core of the rotor and only a small torque is exerted directly on the coil."

Peter's Comments:
- Supports Point 1 (torque acts primarily on iron vs conductor) and point 2 (total force for conductor/slot is the same as the force that the conductor would experience if it directly were in the airgap flux).

End of Excerpt from Reference 25

Excerpt from Reference 26 - "Induction Machine Handbook", by Boldea, Ion and Nasar, Syed,CRC Press, Boca Raton, FL, 2002

"The electromagnetic traveling field produced by the stator currents exists in the airgap and crosses the rotor teeth to embrace the rotor winding Figure 2.16. Only a small fraction of it radially traverses the top of the rotor slot which contains conductor material. It is thus evident that, with rotor and stator conductors in slots, **there are no main forces experienced by the conductors themselves.** Therefore, the method of forces experienced by conductors in fields [F=q*(v x B)] does not apply directly to rotary IMs with conductors in slots...

"It is thus evident that, with rotor and stator conductors in slots, *there are no main forces experienced by the conductors themselves. Therefore, the method of forces experienced by conductors in fields [F=q*(v x B)] does not apply* directly to rotary IMs with conductors in slots...

...According to the Maxwell stress tensor theory, at the surface border between mediums with different magnetic fields and permeabilities (mu=mu0 in air, mu <> mu0 in the core), the magnetic field produces forces. The interaction force component perpendicular to the rotor slot wall is...[lots of math]

...*So the tangential forces that produce the torque occur on the tooth radial walls. Despite this reality, the principle of IM is traditionally explained by forces on currents in a magnetic field*. [F=q*(v x B)]

The principle of operation of IMs is related to torque production. By using the Maxwell stress tensor concept it has been shown that, with windings in slots, _the torque (due to tangential forces) is exerted mainly on slot walls and not on the conductors themselves_. Stress analysis during severe transients should illustrate this reality. It may be demonstrated that _the rotor winding in slots can be "mathematically" moved in the airgap and transformed into an equivalent infinitely thin current sheet. The same torque is now exerted directly on the rotor conductors in the airgap. "_

Peter's Comments:
- Supports Point 1 (torque acts primarily on iron vs conductor) and point 2 (total force for conductor/slot is the same as the force that the conductor would experience if it directly were in the airgap flux).

End of Excerpt from Reference 26

Excerpt from Reference **27** - **"**Electric Motors and Drives: Fundamentals, Types, and Applications" By Austin Hughes.

"TORQUE PRODUCTION – Having designed the magnetic circuit to give a high flux density under the poles (Figure 1.8c), we must obtain maximum benefit from it.   We therefore need to arrange a set of conductors on the rotor, as shown in Figure 1.9, and to ensure that conductors under a N-pole (at the top of Fig 1.9) carry positive current (into the paper), while those under the S-pole carry negative current. The force on all the positive conductors will be to the left, while the force on the negative ones will be to the right. A net couple, or torque will therefore be exerted on the rotor, which will be caused to rotate.

Figure 1.9   _Current-carrying conductors on rotor, positioned to maximise torque. The source of the magnetic flux lines (arrowed) is not shown_
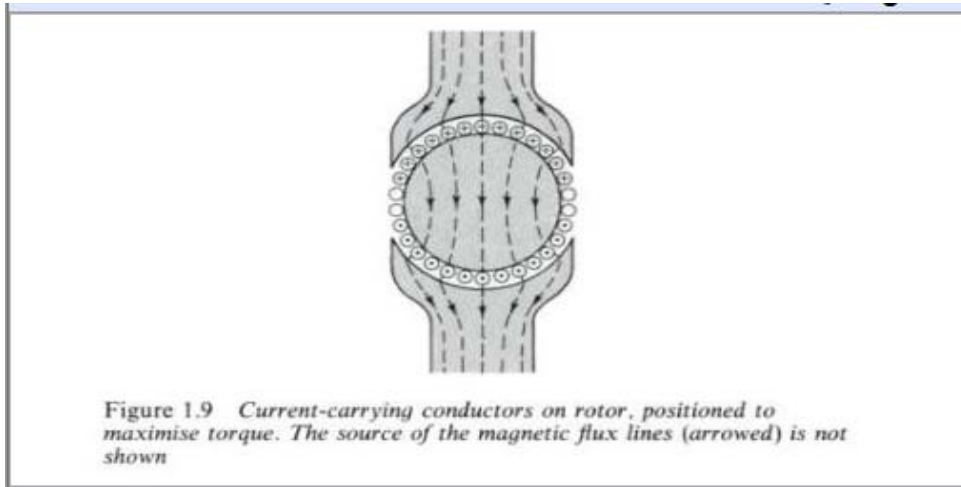
MAGNITUDE OF THE TORQUE – The force on each conductor is given by equation 1.2 [$F=N*L*I*B$], and it follows that the total tangential force F depends on the flux density produced by the field winding, the number of conductors on the rotor, the current in each, and the length of the rotor. The resultant torque (T) depends on the radius of the rotor (r), and is given by $T=F*r$.

SLOTTING – If the conductors were mounted on the surface of the rotor iron, as in Figure 1.9, the air-gap would have to be at least equal to the wire diameter, and the conductors would have to be secured to the rotor in order to transmit their turning force to it. The earliest motors were made like this, with string or tape to bind the conductors to the rotor. We can avoid the penalty of the large air-gap (which results in an unwelcome high reluctance in the magnetic circuit) by placing the conductors in slots in the rotor, as shown in Figure 1.10.
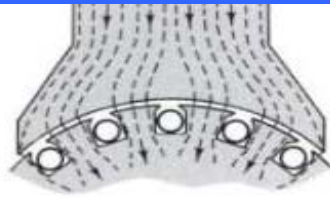
Figure 1.10   Influence on flux paths when the rotor surface is slotted to accommodate conductors

With the conductors in slots, the air-gap can be made small, but, as can be seen from Figure 1.10, almost all the flux now passes down the low-reluctance path through the teeth, leaving the conductors exposed to the very low leakage flux density in the slots. It might therefore be expected that little or no force would be developed, since on the face of it the conductors are screened from the flux**. Remarkably, however, what happens is that the TOTAL FORCE REMAINS THE SAME AS IT WOULD HAVE BEEN IF THE CONDUCTORS WERE ACTUALLY IN THE FLUX, but almost all the force now acts on the rotor teeth, rather than on the conductors themselves.**

This is very good news indeed. By putting the conductors in slots, we simultaneously reduce the reluctance of the magnetic circuit, and transfer the force to the rotor iron, which is robust and well able to transmit the resulting torque to the shaft."

Peter's comments:
- His discussion includes mention that the flux in the slot is very low which leads to his conclusion that force does not act primarily on the conductors.
- Supports Point 1 (torque acts primarily on iron vs conductor) and point 2 (total force for conductor/slot is the same as the force that the conductor would experience if it directly were in the airgap flux).
- Supports Bslot << Bgap

The above portions of this book can be accessed for FREE on-line.
1 – go to www.books.google.com
2 – search for "Electric Motors and Drives: Fundamentals, Types, and Applications"
3 – When results arrive, click on the link for "Electric Motors and Drives.."
4 – close popup window if applicable
5 – Drag scroll bar to view pages 15 through 17

End of Excerpt from Reference **27**

Excerpt from Reference 28 - On-line electromagnetics course, Chapter 6 - Motor Dynamics by G2 Consulting, George P. Gogue, Ph.D· (http://www.consult-g2.com/course/chapter6/chapter.html)

"6.1.1 Forces between a conductor and steel:
The forces on the sides of a deep parallel-sided slot and on the sides of an air-gap can be determined using Maxwell stresses, as shown below.
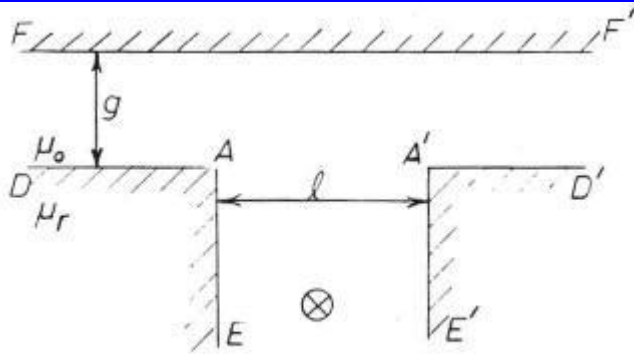
Figure 6.3: A deep slot and air-gap

..[Math deleted]..

.....This **simplified** analysis shows that **the force is actually developed on the sides of the slot rather than directly on the conductor. This explains the paradox that the conductor being in the slot can only see a very small amount of flux to explain the forces (and torque) generated by motors,** (Reference 10).

An alternative physical interpretation can also be used in the generation of force. The main magnetic field causes Ho and Hf at the iron surfaces. The current carrying conductors, however, while carrying current, weaken the field on one side of the slot and strengthen it on the other. The net result is a pull in one direction resulting in rotational torque, (Reference 18). "

Ref 10 Hague, "The Principles of Electromagnetism Applied to Electric Machines", Dover, NY, original 1929, reprinted 1962.
Ref 18. E. B. Maullin, "Electromagnetic Principles of the Dynamo", Oxford, 1955

Peter's comments:
- This particular math proof is very difficult to follow (I did not understand it). But the conclusions are consistent with mine.
- Supports Point 1 (torque acts primarily on iron vs conductor) .

End of Excerpt from Reference 28

Excerpt from Reference 29 - "Finite Element Methods in Electrical Power Engineering" By A.B. J. Reece, T. W. Preston. Published in Electrical Insulation Conference, 1997, and Electrical Manufacturing & Coil Winding Conference Proceedings

"6.1.1 – THE LORENTZ FORCE (OR B L I) [F=NLIxB] METHOD
This straightforward method can be used to establish the magnitude and direction of the force intensity (and hence total force) acting on a conductor or a coil. Where a coil is entirely in air, but interacting with iron components, the computed force will, of course, be equal in magnitude but opposite in direction to the force on the iron.
Force intensity (N/m^2 of [cross] section) is obtained by multiplying the axis components of B from the finite element study by the current density normal to the cross section

considered. The total force is obtained by interaction.

In devices such as the induction motor, with stator and rotor windings in slots, the torque-producing force on the conductors is very small (though the force acting towards the slot bottom may be large). As discussed by, for example Carter (1962), the bulk of the torque forces act on the sides of the teeth.

Peter's comments:
- Supports Point 1 (torque acts primarily on iron vs conductor) and Point 3 (the electromagnetic force that does act on the conductor under load is primarily in the radial direction).

The above portions of this book can be accessed for FREE on-line.
1 – go to www.books.google.com
2 – search for "Finite Element Methods in Electrical Power Engineering"
3 – When results arrive, click on the link for "Finite Element Methods.."
4 – close popup window if applicable
5 – Drag scroll bar to view pages 68

End of Excerpt from Reference 29

Excerpt from Reference 31 - "Analysis of the Mechanical Stresses on a Squirrel Cage Induction Motor by the Finite Element Method", by Chang-Hoon Juri and Alain Nicolas, from IEEE TRANSACTIONS ON MAGNETICS, VOL. 35, NO 3, MAY 1999.

"Therefore, *the flux pass the bars mainly in tangential direction of rotor axis*. The *magnetic forces* have perpendicular direction to the flux path. And so, *their radial components are much greater than the tangential components*. By the direction of J and B, the magnetic forces have the centripetal direction instead of centrifugal direction, with a little tangential component".
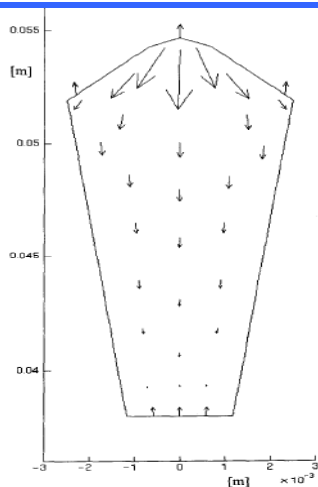
"Fig. 2 The distribution of the magnetic forces in one rotor bar at the moment the forces become maximum, compared with centrifugal forces on the sides of the bar (1200rpm, 20% slip)"

Radial Direction

Tangential Direction

Centrifugal forces (radially outward)
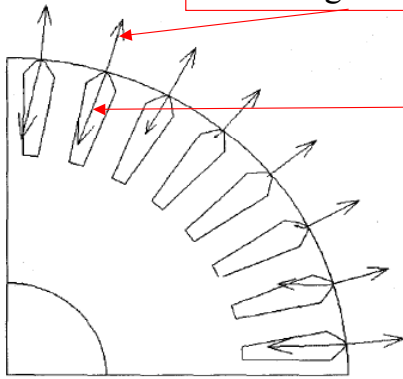
Magnetic Forces (radially inward). Variation follows 4-pole pattern

Figure 1 - Distribution of magnetic and centrifugal forces on the near regions of the airap (1383 rpm, 7.8% slip)

The distribution of the magnetic and centrifugal forces
ᵊ near regions to the airgap (1383 rpm, 7.8 % slip)

Peter's comments
- Note that the inward forces shown in figure 1 are a single vector representing the total of the distributed forces shown in figure 2.
- Supports Point 3 (the electromagnetic force that does act on the conductor under load is primarily in the radial direction).

More complete excerpts from this article can be seen at
http://home.comcast.net/~electricpete1/torque_web/attach/LinkToradialmagforceonbar.htm

End of Excerpt from Reference 31

Excerpt from Reference 32 - "Investigation of High Voltage Stator Winding Vibrations in Faul-Scale Slot Model." by Viktor Kogan and Beant Nindra National Electric Coil Company, L.P.

INVESTIGATION OF HIGH VOLTAGE STATOR WINDING VIBRATIONS IN FULL-SCALE SLOT MODEL

Viktor Kogan and Beant Nindra
National Electric Coil Company, L.P.
Brownsville, Texas---------------Columbus, Ohio

Abstract

This paper represents an approach to a high voltage stator winding vibration in slots evaluation using specially designed full-scale slot model.

one of the spring type elements, has been considered and investigated.

Measurements of the slot model teeth vibration are also presented and discussed. The results obtained by this investigation allowed us to re-evaluate the significance of

3. Brief Theoretical Consideration

3.1 Magnetic Field in Slots. A magnetic field distribution (flux density's graph) along the slot model height is shown in Fig. 3: a- for currents flowing in the same direction, b- for currents flowing in the opposite direction. Three possible field distribution graphs for a real 3 phase machine are shown in Fig. 4. The following conclusions can be made by Fig. 3 and Fig. 4 comparison:

- the radial component of the electromagnetic force rising in a "single phase" slot model is practically equal to the same component in 3 phase winding.
- in the case of opposite current directions the radial component of force in the model is rather less than in the 3 phase generator;

I - coil current, RMS, Amps
b_s - slot width,   cm

For the particular magnetic circuit and winding design of 220 MVA - turbogenerator the following relations were obtained - See Table 1.

Electromagnetic Force Component Relation
(for 220MVA Turbogenerator Design)

Bar Position In Slots	EMF Component Directions	Component's Value in Relative Units (%)	
		Non-saturated Magnetic Circuit	Operational Saturation of Magnetic Circuit
Top	Radial	109	100
	Circumferential	3.2	9.4
Bottom	Radial	36	33.7
	Circumferential	1.2	8

Peter's comments:
- The table above shows radial component if 4 - 30 times larger than the circumferential (tangential) component of force on the conductor.
- The authors were specifically studying force on the conductors (roebel bars).
- This was a single phase experimental fixture. Authors concluded it was similar to actual machine forces.
- <u>Supports</u> Point 3 (the electromagnetic force that does act on the conductor under load is primarily in the radial direction).

End of Excerpt from Reference 32

Excerpt from Reference 33 - "Slot Discharge Mechanisms In High Voltage Rotating Machines" by D G Edwards of The Robert Gordon University, UK

"Electromagnetic forces tend to induce various modes of vibration in a stator winding. **<u>Within the slot section of the winding the primary forces are radial </u>and tight wedging is necessary to prevent movement**. If the slot wedges become loose then there is a risk of physical damage to the coil insulation, and eventual failure, due to abrasion and impacting against the sides and bottom of the slot. An early consequence of physical abrasion is damage to the corona screen and this results in a rapid change in the partial discharge characteristic which, if correctly interpreted, may enable corrective action to be taken before the damage becomes severe."

Peter's comments:
- <u>Supports</u> Point 3 (the electromagnetic force that does act on the conductor under load is primarily in the radial direction).

End of Excerpt from Reference 33

Excerpt from Reference 34 - "Measures and Technologies to Enhance the Insulation Condition Monitoring of Large Electrical Machines", by J. Keith Nelson and Saber Azizi-Ghannad, IEEE Transactions on Dielectrics and Electrical Insulation Vol. 11, No. 1; February 2004

"A single conductor of dimensions h, x, w carrying a current I completely filling a stator

slot will be accompanied by a leakage flux density, Bx which is normal [tangential] to the slot and increases as the distance, x, outwards from the bottom of the slot:

Bxs = μ0 * Ix / (h*w)

The cross product of this leakage flux and the load creates a Lorentz force at twice supply frequency which acts to compress the insulation <u>towards the bottom of the slot.</u>

Peter's comments:
- This author is saying the direction of flux is tangential and the resulting direction of force on the conductor is radial (towards the bottom of the slot).
- If the torque producing force acted on the conductor, surely a paper addressing insulation condition would address the compressive effects of the torque acting on the insulation on the side of the slot.
- <u>Tends to supports</u> Point 3 (the electromagnetic force that does act on the conductor under load is primarily in the radial direction), although this reference in itself is not conclusive.

End of Excerpt from Reference 34

Excerpt from Reference 35 - EPRI TR 5036 (Power Plant Electrical Reference Series), Volume 16 ("Handbook to Assess the Insulation Condition of Large Rotating Machines")

"3.3.2.1 – '120-Hz Bar Vibration Forces' – The current in each stator slot produces a *<u>cross-slot flux</u>* [tangential] which *acts on the conductors in that slot to produce a force that is generally toward the bottom of the slot"* [RADIAL DIRECTION]

Peter's Comment:
- <u>Supports</u> Point 3 (the electromagnetic force that does act on the conductor under load is primarily in the radial direction).

End of Excerpt from Reference 35

Excerpt from Reference 36 - "Electrical Insulation For Rotating Machines" By Greg Stone, Edward A. Boulter, Ian Culbert, And Hussein Dhirani ISBN 0-471-44506-1

"Mechanical Design. There are large magnetic forces acting on the copper conductors. These magnetic forces are primarily the result of the two magnetic fields from the current flowing in the top and bottom coils/bars in each slot. These fields interact, exerting a **force that makes the individual copper conductors as well as the entire coil or bar vibrate (primarily) up and down in the slot.** The force, F, acting on the top coil at 120 Hz for a 60 Hz current in the radial direction for 1 meter length of coil is given by [1.12]:

$$F = k*I^2/d \text{ kN/m (1.3)}$$

where I is the rms current through the Roebel bar, or I = nI0, with I0 being the rms coil current times the number of turns in the coil; d is the width of the stator slot in meters; and k is 0.96. The force is expressed in kN of force acting per meter length of coil/bar in the slot. If the current in a stator bar is

I = A sin wt

where w is 2Pif, f is the 50 or 60 Hz power frequency, and t is time. Then (1.3) becomes

$$F = k A^2 * (1-cos(2*w*t))/(2d)$$

Thus, there is a net force to the bottom of the slot. Around this "DC" force is an oscillating force at twice the power frequency, i.e., 100 Hz or 120 Hz. T**here is also a 100 or 120 Hz force in the circumferential direction caused by the rotor's magnetic field interacting with the current in the stator coil/bar. <u>This circumferential force is only about 10% of the radial force</u>**"

[1.12]"

....1.12 J. F. Calvert, "Forces in Turbine Generator Stator Windings," Trans of AIEE, 1931, pp. 178–196.

Peter's Comments
<u>Supports</u> Point 3 (the electromagnetic force that does act on the conductor under load is primarily in the radial direction).

End of Excerpt from Reference 36

Section 23 About the author

Peter has a BSEE from the University of Rochester (1987), a Master of Engineering Administration in Industrial/Systems Engineering from Virginia Polytechnic Institute and State University (1993), a MSEE from Georgia Institute of Technology (2000), and a Professional Engineer's license granted from the state of Texas by examination. He has over 20 years of experience in the area of power plant electrical systems and equipment. He has been the electric motor engineer at the South Texas Project nuclear plant since 2000.

Peter is an active participant at the condition monitoring forums at maintenanceforum.com (username: electricpete).   Readers are invited to contact him with questions or comments at the maintenanceforums.com motor forum, or by email: electricpete@technologist.com .

Thanks to Jan Krepela for his insight in this topic.